New middle and late Smithian ammonoid faunas from the Utah/Arizona border: new evidence for calibrating Early Triassic transgressive-regressive trends and paleobiogeographical signals in the western USA basin.

Arnaud Brayard, Nicolas Olivier, Emmanuelle Vennin, James F. Jenks, Kevin G. Bylund, Daniel A. Stephen, Dawn Mcshinsky, Nicolas Goudemand, Emmanuel Fara, Gilles Escarguel

New middle and late Smithian ammonoid faunas from the Utah/Arizona border: new evidence for calibrating Early Triassic transgressive-regressive trends and paleobiogeographical signals in the western USA basin

Arnaud Brayard [1,*], Nicolas Olivier [2], Emmanuelle Vennin [1], James F. Jenks [3], Kevin G. Bylund [4], Daniel A. Stephen [5], Dawn McShinsky [6], Nicolas Goudemand [7], Emmanuel Fara [1], Gilles Escarguel [8]

[1] Biogéosciences, UMR6282, CNRS, Université Bourgogne Franche-Comté, 6 Boulevard Gabriel, 21000 Dijon, France

[2] Université Clermont Auvergne, CNRS, IRD, Laboratoire Magmas et Volcans, 63000 Clermont-Ferrand, France

[3] 1134 Johnson Ridge Lane, West Jordan, Utah 84084, USA

[4] 140 South 700 East, Spanish Fork, Utah 84660, USA

[5] Department of Earth Science, Utah Valley University, 800 West University Parkway, Orem, Utah 84058, USA

[6] 7202 Yardley Drive, Katy, Texas 77494, USA

[7] Université de Lyon, ENS de Lyon, CNRS, Université Claude Bernard Lyon 1, Institut de Génomique Fonctionnelle de Lyon, UMR 5242, 46 Allée d'Italie, 69364 Lyon Cedex 07, France

[8] Univ. Lyon. Laboratoire d'Ecologie des Hydrosystèmes Naturels et Anthropisés, UMR 5023 CNRS, Université Claude Bernard Lyon 1, ENTPE. F-69622 Villeurbanne Cedex, France

*Correspondence to: arnaud.brayard@u-bourgogne.fr

Abstract

New Smithian (Early Triassic) ammonoid assemblages were sampled near the Utah/Arizona border. They provide several spatiotemporal constraints on the regional Sinbad Formation showing that the extent of the Smithian sea in the southwestern-most part of the western USA basin is larger than previously expected, reaching northern Arizona and an area just east of Kanab in Kane County, Utah. This southwestern-most excursion of the sea in the western USA basin is part of the third order Smithian transgression-regression cycle, which is well-documented worldwide. These new spatiotemporal constraints also indicate that the Sinbad Formation spans the late middle to early late Smithian time interval in the studied area. The observed transgressive trend corresponds to the warm temperatures of the middle-early late Smithian and the regressive trend to the cooling phase spanning the Smithian-Spathian transition. Thus, the Sinbad Formation and its marine deposits are the direct result of global climatic fluctuations and related sea-level changes that occurred from the late middle Smithian to the Smithian-Spathian transition. This highlights the importance of the Sinbad Formation in untangling local and global changes occurring around the late Smithian, and thus in overcoming a major obstacle to the understanding of the biotic recovery after the Permian/Triassic boundary mass extinction. This also indirectly confirms that the western USA basin is a key area containing essential information for the understanding of the Early Triassic events. The taxonomic richness of late middle Smithian assemblages is much lower in the studied area than in the more northern localities. However, the occurring taxa confirm the known regional to global distribution of Smithian ammonoids, witnessing the major global environmental changes from the middle Smithian to the early Spathian.

Keywords:

Smithian, Early Triassic, Ammonoids, Utah, Arizona, Biostratigraphy, Transgression-regression cycle

1. Introduction

Our understanding of the complex biotic rediversification that occurred in the first million years after the Permian/Triassic boundary mass extinction (PTBME; ca 251.9 Ma, Baresel et al., 2017) requires detailed sedimentological studies to reconstruct depositional environments and their evolution (Bagherpour et al., 2017; Kershaw, 2017; Olivier et al., 2018). Indeed, the type of depositional settings as well as sea-level changes directly influences how the nature and preservation of the fossil record is to be analyzed and interpreted (Brett, 1995; Behrensmeyer et al., 2000). However, deciphering the spatiotemporal variation patterns of Early Triassic depositional environments requires calibrating the sedimentary record according to a biostratigraphically-controlled accurate timescale (Brühwiler et al., 2010; Ware et al., 2015; Brosse et al., 2016).

The Early Triassic is characterized by a global long-term sea-level rise with several second- and third-order transgressive-regressive sequences that can be identified worldwide (Embry 1988; Haq and Al-Qahtani, 2005; Haq, 2018). The western USA basin, mainly covering present day eastern Nevada, Utah, Idaho and western Wyoming (**Fig 1A, B**), is one of the few places where these sequences can be recognized, and it includes a notable third order transgressive-regressive cycle dated from the Smithian substage (Collinson and Hasenmueller, 1978; Clark and Carr, 1984; Paull and Paull, 1993, 1997; Embry, 1997; Lucas et al., 2007b; Brayard et al., 2013; Olivier et al., 2014, 2016, 2018; Vennin et al., 2015; Jeffrey et al., 2019). A rapid transgression towards the south and south-east is recorded within

the southern part of the western USA basin during the early-middle Smithian (**Fig. 1C**), followed by a marked regression near the Smithian/Spathian boundary (Paull and Paull, 1993, 1997; Lucas et al., 2007b; Brayard et al., 2013). However, the southern-most boundary of the late Smithian sea is difficult to establish. Several contributions briefly reported on the presence of undetermined and poorly-preserved gastropods, bivalves and ammonoids (Gregory, 1948, 1950; Blakey, 1979; Doelling and Davis, 1989) as well as scarce conodonts (e.g., Paull and Paull, 1993; Lucas et al., 2007b) from several localities in southern Utah. These organisms served for instance to characterize local open marine conditions, but the associated timescale was poorly constrained.

Newly-found Smithian ammonoid faunas near the Utah/Arizona border allow us to determine a more accurate minimal age for the arrival of the open sea in the southern-most part of the western USA basin. Additionally, in well-characterized depositional settings, these faunas allow us to constrain the minimum duration of the corresponding stratigraphic units. For the first time, we also report late middle and late Smithian ammonoid assemblages from northernmost Arizona demonstrating that the Smithian transgression reached this area as soon as the late middle Smithian. Finally, these new ammonoid assemblages support the severe biotic and climatic fluctuations known from the middle Smithian to the early Spathian in both, the western USA basin and worldwide, highlighting that this basin encompasses various exposures that can provide invaluable insights into the mechanisms underlying these major events in the aftermath of the PTBME (Schubert and Bottjer, 1995; Goodspeed and Lucas, 2007; Pruss et al., 2005, 2007; Mata and Bottjer, 2011; Hofmann et al., 2013, 2017; Brayard et al., 2017).

2. Early Triassic basinal setting

During the Early Triassic, the western USA basin was located within the northern intertropical zone of the western margin of Pangea (**Fig. 1A, B**) and recorded both terrestrial and marine deposits (Moenkopi and Thaynes groups, respectively; *sensu* Lucas et al., 2007b). This epicontinental basin was contemporaneous with the Sonoma orogeny and is usually interpreted as a foreland basin (Stewart et al., 1972; Collinson et al., 1976; Dickinson, 2013; Caravaca et al., 2018). It presently covers large areas within eastern Nevada, Utah, Idaho, western Wyoming and southwestern Montana. The southern part of the basin records Smithian and Spathian marine deposits, whereas an earlier portion of the Early Triassic is documented in the northern part (e.g., McKee, 1954; Kummel, 1957). Based on a reappraisal of lithology, thickness and subsidence rates, as well as on quantitative biogeographical analyses of ammonoids within the basin, Caravaca et al. (2018) and Jattiot et al. (2018) showed a marked north-south differentiation of the western USA basin in terms of organism distribution and tectonics. On the latter point, the southern part of the basin shows a relative quiescence during the Early Triassic and can be considered more stable and much less influenced by short-term tectonic deformations than the northern part, mostly likely due to the stronger rigidity inherited from its basement terranes (Caravaca et al., 2018). Recently published carbon and sulfur isotope curves from several localities within this basin (Thomazo et al., 2016, 2019; Caravaca et al., 2017; Schneebeli-Hermann et al., 2020) show that the well-known global isotopic signals were markedly influenced by local processes resulting from environmental and biotic heterogeneities within the basin during the Early Triassic.

3. Previous Smithian-early Spathian stratigraphic framework in southern Utah and recent developments

In the southern part of the western USA basin, and mainly in southern Utah, depositional settings correspond to relatively shallow environments (tidal to outer shelf; **Fig. 1C**) characterized by shale and limestone sediments. Marine facies deposited during the early-middle Smithian transgression are typical and are generally represented by various microbial deposits overlain by, or interfingered with, bioclastic limestones (Lucas et al., 2007a, b; Goodspeed and Lucas, 2007; Brayard et al., 2011, 2013; Mata and Bottjer, 2011; Olivier et al., 2014, 2016, 2018; Vennin et al., 2015; Jeffrey et al., 2019). The often-massive microbial deposits exhibit complex metazoan consortia including sponges and bivalves, forming laterally discontinuous bioconstructions (e.g., Brayard et al., 2011; Olivier et al., 2018). Bioclastic limestones generally contain various organisms such as ammonoids, bivalves, gastropods, echinoderms and lingulid brachiopods (Brayard et al., 2013, 2015; Olivier et al., 2014, 2018). These microbial-bioclastic deposits are documented at many places in southern Utah and correspond to the Timpoweap and Sinbad fms. The Timpoweap Fm. is now considered as a junior synonym of the Sinbad Fm. (Lucas et al., 2007b).

In southwestern-most Utah, e.g., in the Hurricane area (**Figs. 1D, E; 2**), the Sinbad Fm. overlies the Rock Canyon Conglomerate of uncertain age, which represents the hiatus in marine deposits that lasted from the Late Permian to the beginning of the Early Triassic. This formation is made of various breccias and thick channelized conglomerates that may fill incised valleys in the Permian Kaibab Fm. (e.g., Blakey, 1979; Marzolf, 1993; Olivier et al., 2014, 2018). A facies gradation between conglomerates and microbial deposits is often visible between the Rock Canyon Conglomerate and the Sinbad Fm. (Nielson, 1991; Olivier et al., 2014, 2018), suggesting that they belong to the same stratigraphic unit and that the Rock Canyon Conglomerate may therefore be Early Triassic in age.

Previous works in southern Utah merely mentioned the occurrence in the Smithian Timpoweap Fm. of e.g., "*Meekoceras*" (Reeside and Bassler, 1922; Reeside, 1943; Gregory,

1948, 1950; Stewart et al., 1972; Nielson and Johnson, 1979; Nielson, 1991), a long-ranging Smithian ammonoid genus, which can be easily confused with many other genera when poorly preserved (Brayard et al., 2013), potentially leading to biostratigraphical mistakes or confusion. Additionally, these reports were often diluted or repeated in different studies (e.g., Doelling and Davis, 1989). More recently, Lucas et al. (2007b), Brayard et al. (2013) and Olivier et al. (2014, 2018) identified typical late Smithian assemblages in different localities of southwestern Utah. These reports indicated that the transgression had already reached southwestern Utah during the middle Smithian and southwestern-most Utah (Hurricane area) at least during the late Smithian.

The age of the Sinbad Fm. is therefore constrained by the occurrence of typical late Smithian ammonoid genera such as *Anasibirites* and *Wasatchites* in its uppermost layers (Lucas et al., 2007b; Brayard et al., 2013; Olivier et al., 2018; Jeffrey et al., 2019). Conodonts also indicate a late Smithian age for these beds (Lucas et al., 2007b; Olivier et al., 2014). Typical latest Smithian ammonoid assemblages in which e.g., *Pseudosageceras augustum*, *Xenoceltites* and *Glyptophiceras* can co-occur (Brayard et al., 2013; Jattiot et al., 2017, 2018; Jenks and Brayard, 2018) have not yet been found in southwestern-most Utah, suggesting that a rapid regressive phase was probably already occurring at that time in this area. Age constraints for the base of the Sinbad Fm., i.e. the microbially-dominated part, are much vaguer due to, e.g., the paucity and poor preservation of conodonts (Paull and Paull, 1993). However, a middle Smithian ammonoid, *Owenites* sp., was recently reported from the top of microbial fenestral deposits in the Timpoweap Canyon near Virgin (Olivier et al., 2014). The age of the base of the Sinbad Fm. in other localities within the Hurricane area is yet to be determined.

The Sinbad Fm. is stratigraphically covered by the Lower Red Member, which marks a regressive trend during the Smithian-Spathian transition, showing a marginal and terrestrial sedimentation (Blakey, 1979; Lucas et al., 2007b). A new marine incursion is recorded by the

overlying Virgin Limestone Fm., which is early Spathian in age (Poborski, 1954; Hautmann et al., 2013; Hoffmann et al., 2013).

4. Studied exposures and sampled material

Ammonoid specimens studied herein were collected from four localities near the Utah/Arizona border where the Sinbad Fm. is exposed: two in Washington County, Utah (Workman Wash and Honeymoon Trail); one in Kane County, Utah (White Sage Wash); and one in Rock Canyon, Mohave County, Arizona (**Fig. 1D-F**). Ammonoid preservation in some cases is quite good, with some shell remains preserved, for instance in Workman Wash. However, internal recrystallization is common, making the collection and preparation of these specimens often difficult. Also, exposing suture lines is often impossible.

The Workman Wash locality (**Figs. 1D, E, 2**; 37°5'56.96"N, 113°17'31.01"W) was described in detail by Olivier et al. (2018). Unlike many other exposures of the Sinbad Fm. in the area, it exhibits contemporaneous fossiliferous lateral deposits of the microbially-dominated unit. This unit also displays moderately-diversified faunal assemblages that can be traced laterally from microbial to the bioclastic deposits. Within the assemblages of the microbially-dominated unit, ammonoids and large-sized gastropods are abundant (Brayard et al., 2015). Ammonoids, often accumulated in large lenses and specific beds, are represented by typical early late Smithian prionitid genera such as *Anasibirites*, *Wasatchites*, *Gurleyites* (specimens previously attributed to *Arctoprionites* in the western USA basin) and *Hemiprionites*. Contrary to many other localities in the western USA basin, *Gurleyites smithi* (ex-"*Arctoprionites resseri"*) specimens sampled in Workman Wash are abundant and well preserved, exhibiting a very large intra-specific variation and unexpected ornamentation. These features have not yet been observed in specimens from other localities and they provide

new information for prionitid taxonomy and systematics (see Systematics section). Middle Smithian ammonoid taxa have not yet been found at Workman Wash, indicating that the open sea possibly did not reach this locality until the early late Smithian. A neighboring exposure with an identical name, but located in a more northern canyon, was recently described by Jeffrey et al. (2019) and shows a similar succession. However, no ammonoids were reported from this site, preventing further in-depth biostratigraphical comparisons.

The second southern Utah site studied herein is located along a ~500 m gully on the eastern edge of the Honeymoon Trail, bordering the Hurricane Cliffs (**Fig. 1D, E**; 37°1'42.93"N, 113°16'16.44"W). Only the topmost part of the Rock Canyon Conglomerate and the basal microbially-dominated part of the Sinbad Fm. are visible here (**Fig. 2**). Our observations confirmed the brief report by Perfilli and Ritter (2018), who indicated that large microbial mounds are well exposed at this site and are made of various microbial deposits. These microbial limestones also contain abundant 1-6 cm-high gastropod shells (possible *Coelostylina* sp.) and common late middle Smithian ammonoids, such as *Inyoites* and *Guodunites*, often densely packed into dm-scale lenses. A few sphaeroconic (*Juvenites* or *Paranannites*) and serpenticonic (*Dieneroceras*?) ammonoids rarely occur, but they are too poorly preserved for firm determination. Jeffrey et al. (2019) described a neighboring section ("Cottonwood Wash"; ~700 m to the SW) where the Sinbad Fm. is well exposed but they did not report ammonoids from the microbially-dominated unit.

The third studied site is located at the wash entrance of Rock Canyon, in Mohave County, northernmost Arizona, just south of the Utah border (**Figs. 1D, E, 3**; 36°58'43.35"N, 113°15'37.67"W). The Rock Canyon Conglomerate is well developed, showing thick channelized conglomerates filling large incised valleys. This site serves as a type section for this formation (Reeside and Bassler, 1922; Nielson, 1991). Overlying microbial deposits of the Sinbad Fm. are also well exposed and include abundant large gastropods (Brayard et al.,

2015) and two successive ammonoid assemblages. The lowermost assemblage is monogeneric and contains the late middle Smithian *Guodunites hooveri* and *G. monneti*, whereas the uppermost assemblage includes early late Smithian taxa such as *Anasibirites*. Ammonoid occurrences at the same site were also reported by Nielson (1991) and Jeffrey et al. (2019), but without firm identification and detailed biostratigraphic zonation.

The fourth studied site is White Sage Wash, located ~25 km east of Kanab and ~200 m north of the Utah/Arizona border (**Fig. 1D, F**; 37°0'12.84"N, 112°13'51.60"W). Lower Triassic rocks are relatively widespread in Kane County, but developed exposures of the Sinbad Fm. are rarely investigated in detail (but see Jeffrey et al., 2019 for a recent study of two neighboring localities in the Buckskin Mountains). In addition, occurrences of Smithian ammonoids east of Kanab were neither firmly identified (e.g., Gregory, 1948) nor even reported from the Sinbad Fm. in this area (Doelling and Davis, 1989; Jeffrey et al., 2019). Only part of the microbially-dominated unit of the Sinbad Fm. is visible at the studied site (**Fig. 3**), but we can reasonably assume that the local Early Triassic succession is similar to those observed at neighboring sites (Jeffrey et al., 2019). Total exposed strata (only ~4.5 m thick) consist of various microbial deposits that tend to locally form small wavy mounds. Ammonoids and large gastropods (e.g., *Coelostylina* sp. A, *Abrekopsis*, ?*Worthenia*) are abundant and often clustered in lenses, as already noted by Reeside (1943) and Gregory (1948) in some neighboring exposures. Three successive ammonoid assemblages were found at this site and all contain late middle Smithian *Guodunites hooveri*. Additionally, the uppermost assemblage contains a rather evolute taxon that is too poorly preserved to be firmly identified, but it resembles the middle Smithian genus *Dieneroceras*.

5. The Smithian sea near the Utah/Arizona border: arrival, duration, extent, and correlation

5.1. Biostratigraphical significance of sampled ammonoids

A total of eight ammonoid taxa were identified from the four studied localities. These are attributed to specific ammonoid zones permitting high-resolution correlation at a local to global scale (Brayard et al., 2009a, 2013; Jenks et al., 2010, 2015; Jattiot et al., 2017; Jenks and Brayard, 2018).

Inyoites oweni was found at a single locality, Honeymoon Trail, indicating the presence of the late middle Smithian *Inyoites* horizon, which is widely found in the southern part of the basin at the top of the *Owenites* beds (e.g., Brayard et al., 2013) and at several places worldwide (Jenks et al., 2015). It co-occurs with *Guodunites hooveri*, which is abundant throughout the studied area. This taxon is restricted to the *Inyoites* horizon and is thus characteristic of the late middle Smithian in the southern part of the basin (Brayard et al., 2009a, 2013; Stephen et al., 2010) and the top of the regional middle Smithian UAZ4 as defined by Jattiot et al. (2017). Although rare, *Guodunites* also occurs in late middle Smithian assemblages of the *Owenites* beds at Crittenden Springs, NE Nevada (Jenks and Brayard, 2018). Additionally, *Guodunites* is typically found in late middle Smithian ammonoid assemblages in Oman (Brühwiler et al., 2012a), Vietnam (Shigeta et al., 2014) and South China (Brayard and Bucher, 2008). These new findings are also consistent with the report of the occurrence of *Owenites* sp. in the Sinbad Fm. at the more northern locality of Virgin Dam (Olivier et al., 2014).

In the more complete sections at Workman Wash and Rock Canyon, sampled ammonoids in the upper part of the Sinbad Fm. correspond to the typical prionitid assemblage of early late Smithian age. This assemblage includes the cosmopolitan genera *Anasibirites* and *Wasatchites*, and is found throughout the basin (e.g., Brayard et al., 2013; Jattiot et al., 2017,

2018) and also worldwide (see Jenks et al., 2015 for global correlations). It corresponds to the regional UAZ5 as defined by Jattiot et al. (2017). Typical latest Smithian ammonoid taxa such as *Xenoceltites, Glyptophiceras* and *Pseudosageceras augustum* were not found in the uppermost beds of the Sinbad Fm. likely indicating that the sea had already receded from the area by this time.

5.2. Richness and abundance of sampled ammonoids

Although relatively abundant in all studied localities, ammonoids show a very low taxonomic diversity compared to the more northern localities in the basin (Brayard et al., 2013; Jattiot et al., 2017, 2018; Jenks and Brayard, 2018), with the richest assemblages mainly recorded during the late Smithian. Late middle Smithian ammonoids such as *Guodunites* or *Inyoites* are typical of the southern part of the basin (e.g., Jattiot et al., 2018); it is therefore not surprising to find them near the Utah/Arizona border. Unexpectedly, some taxa typical of the middle Smithian in this part of the basin, such as *Churkites*, or more cosmopolitan taxa, such as *Meekoceras gracilitatis*, are supposedly absent. This is striking, because although often reported from the studied area, the iconic *M. gracilitatis* was actually probably misidentified (see Brayard et al., 2013).

The unusual very low richness of late middle Smithian ammonoid assemblages in the southwestern-most part of the basin can be explained by the shallow seas in this area (mostly peritidal settings) that may have been favorable to only a few taxa. Jattiot et al. (2018) has already pointed out that the distribution of middle Smithian ammonoids within the western USA basin was highly contrasted, both in terms of abundance and richness, according to north-south and south-north gradients. These authors emphasized the role of the terrigenous load, and thus turbidity, in the water column and hydrodynamics in the spatial segregation of

taxa. They suggested that taxa preferentially found in the southern part of the basin (such as *Guodunites*) were more tolerant to higher terrigenous load levels than taxa with northern affinities. Peritidal settings as found in the studied area, and especially recorded in the microbially-dominated unit of the Sinbad Fm., rarely show a high terrigenous load. However, they were potentially more subject to higher temperature and salinity levels than in more northern localities, possibly favoring a few taxa more tolerant to these conditions. There is no strong evidence for taphonomic bias, mechanical sorting or differential transport that could explain why some species appear to occur abundantly in this shallow setting. The combination of (*i*) the observed preservation of shells without damage, and (*ii*) the presence in neighboring areas with similar depositional settings, of diversified ammonoid assemblages including various taxa with morphologies similar to those collected here, better argue for a causal relationship between species paleoecology and local environmental conditions. However, this point deserves further investigation by continuing to explore nearby fossiliferous localities.

Late Smithian ammonoid assemblages include highly cosmopolitan taxa (Brayard et al., 2006, 2007). These assemblages are typical and are recognized throughout the basin (Lucas et al., 2007b; Brayard et al., 2013; Jattiot et al., 2017, 2018; Jenks and Brayard, 2018) and worldwide (see Brühwiler et al., 2010; Zakharov and Abnavi, 2013; Shigeta et al., 2014; Jenks et al., 2015; Jattiot et al., 2016 for reviews in different basins). They show a low taxonomic richness and serve to mark the base of the late Smithian. Indeed, they follow a major extinction event at the middle/late Smithian boundary and correspond to the beginning of marked shifts in environmental conditions such as cooling and anoxia (e.g., Grasby et al., 2013; Goudemand et al., 2019; Zhang et al., 2019). On that ground, early late Smithian ammonoid assemblages observed in the southwestern-most USA basin provide an excellent

record of the global environmental fluctuations that took place at that time as they correspond to the warmest temperatures reached during the Smithian-Spathian transition (see section 5.4).

5.3. Local and regional constraints on the Smithian sea

The new ammonoid assemblages from the area near the Utah/Arizona border show that the Smithian sea extended farther south than previously known, reaching northern Arizona and the eastern part of Kane County, Utah. They also indicate that marine deposits corresponding to the Sinbad Fm. span the late middle to early late Smithian interval in this area (**Fig. 4**). Except for the Workman Wash site, the oldest ammonoid assemblages found in the lower beds of the Sinbad Fm. are all of late middle Smithian age. The thin beds that characterize the transition between the Rock Canyon Conglomerate and the Sinbad Fm. are devoid of characteristic fossils, but the proximity of these beds with strata containing late middle Smithian ammonoids as well as the apparent absence of a sedimentation break suggests that they are very close in age. Because the microbial facies of the Sinbad Fm. progressively overlie the Rock Canyon Conglomerate (Nielson, 1991; Olivier et al., 2014), we can hypothesize that at least the upper part of this formation is likely Smithian in age. At Workman Wash, index fossils have not yet been found in the lowermost beds. We therefore cannot confirm a potential late middle Smithian age for these beds or that the open sea reached this locality slightly later than expected, i.e. during the late Smithian.

The age of the Sinbad Fm. at the more northern localities of Cedar City and Kanarraville has been shown to span at least the late middle Smithian and late Smithian (Lucas et al., 2007b; Brayard et al., 2013). Thus, from Cedar City south to the Utah/Arizona border, exposures of the Sinbad Fm. are almost coeval, suggesting a very rapid transgression during this interval. Slightly older strata are probably present in the Cedar City and Kanarraville areas, indicating

that the transgression reached these localities first, but age constraints are still lacking to determine its exact timing (Brayard et al., 2013). Finally, the late middle to late Smithian age of the Sinbad Fm. in the entire southwestern-most region of Utah further justifies the synonymization of the Timpoweap Fm. with the Sinbad Fm. (Lucas et al., 2007b).

5.4. Connections with global climatic and biotic events

Overall, one of the most important pieces of information provided by these new biostratigraphic data is that the advancement of the sea throughout the relatively large studied area, as well as its retreat, was extremely rapid (a time span less than that of an ammonoid zone). The amount of time recorded by the Sinbad Fm. in this area is also rather restricted as it corresponds only to the *Inyoites* horizon-*Anasibirites multiformis* beds interval. If we translate this biostratigraphic interval into an approximate duration based on the present-day estimates provided by Brühwiler et al. (2010) for Smithian ammonoid UA zones, this epicontinental sea likely persisted in the area near the Utah/Arizona border for a period less than 100 kyr. This relatively short-term marine incursion into the southern-most western USA basin is part of the Smithian third order transgressive-regressive cycle, which is known in several basins worldwide (e.g., Paull and Paull, 1997).

During the Smithian, the southern part of the western USA basin exhibited relatively shallow environments and is characterized by a relative tectonic quiescence (Caravaca et al., 2018). In such a context, where regional and global tectonic controls can likely be ruled out (e.g., Olivier et al., 2014; Haq, 2018), the observed transgressive/regressive cycle in the studied area is probably related primarily to climatic changes (Olivier et al., 2014). In the current absence of reported evidence for intermittent high-latitude continental ice-sheets for the Early Triassic, such rapid m-scale eustatic fluctuations may be explained either by the variations in

storage of aquifers and lakes (Hay and Leslie, 1990; Jacobs and Sahagian, 1993; Haq, 2018) or by the thermal expansion and retraction of ocean waters (Gornitz et al., 1982; Schulz and Schäfer-Neth, 1997).

The time interval represented by the Sinbad Fm. is coeval with a dramatic and sudden global climatic change, as it spans the passage from middle Smithian warm temperatures to much colder temperatures during the late Smithian and Smithian-Spathian transition. Warmest temperatures were initially assumed to have occurred at the Smithian/Spathian boundary based on $\delta^{18}O$ conodont data analyzed by conventional gas isotope ratio mass spectrometry (Sun et al., 2012; Romano et al., 2013). Nevertheless, recently published $\delta^{18}O$ conodont data analyzed by sensitive high-resolution ion microprobe indicated that the warmest temperatures were reached during the middle and early late Smithian, followed by a cooling phase during the rest of the Smithian and the Smithian-Spathian transition (Goudemand et al., 2019).The observed transgressive trend therefore corresponds to the middle-early late Smithian warmer temperatures and the regressive trend to the cooling phase spanning the latest Smithian and Smithian-Spathian transition. Thus, the Sinbad Fm. and its marine deposits seem to be the direct result of global climatic fluctuations and related sea-level changes that occurred from the late middle Smithian to the Smithian-Spathian transition.

These climatic and sea-level changes have also been associated with several other environmental perturbations such as changes in carbon and sulfur cycles (Payne, 2004; Horacek et al., 2007b; Galfetti et al., 2007; Song et al., 2014; Zhang et al., 2015; Stebbins et al., 2019; Thomazo et al., 2019) and anoxia (Horacek et al., 2007a; Shigeta et al., 2009; Grasby et al., 2013; Sun et al., 2015; Clarkson et al., 2016; Zhao et al., 2020). They also coincide with a major extinction of nekto-pelagic organisms such as ammonoids and conodonts during the late Smithian (Tozer, 1982; Dagys, 1988; Hallam, 1996; Orchard, 2007; Stanley, 2009; Jattiot et al., 2016). Much caution should be heeded when interpreting the

detailed timing and spatial extent of these perturbations, as well as their underlying causal processes such as volcanism and redox changes (reader can refer to e.g., Hammer et al., 2019 and Thomazo et al., 2019 for recent examples of discussion). Our knowledge of the short late Smithian time interval has improved recently by showing that successive cosmopolitan ammonoid assemblages thrived during this time interval (e.g., Jenks et al., 2015). Mechanisms controlling the major extinction at the middle/late Smithian boundary and the marked dominance of prionitids at the beginning of the late Smithian are still hypothetical, but they probably can be primarily related to the warm temperature reached at that time. Ammonoid assemblages that followed correspond to the cooling phase, finally leading to the installation of the more endemic assemblages of the early Spathian. This change supports a link between ammonoid diversity *s.l.* and distribution, and rapid fluctuations of the latitudinal gradient of sea-surface temperature during the Smithian-Spathian transition (e.g., Brayard et al., 2006). Contemporary changes in other environmental parameters such as redox conditions or continental weathering may have also influenced ammonoid diversity, but their effects are presently much harder to assess (e.g., Jattiot et al., 2018). Thus, the observed sedimentological and paleontological changes recorded in the Sinbad Fm. are consistent with coeval global climatic and biotic events. This also emphasizes that detailed and replicated field studies conducted within a regional sedimentary basin by revealing basin-wide paleontological, sedimentological and geochemical signals and variabilities can provide valuable and meaningful clues to environmental changes and evolutionary processes during a global crisis.

6. Conclusions

New Smithian ammonoid assemblages sampled near the Utah/Arizona border provide for the first time several spatiotemporal constraints on the regional Sinbad Fm. (western USA basin), highlighting its importance for understanding environmental and biotic events during the middle and late Smithian, *ca.* 1 myr after the Permian/Triassic boundary mass extinction. This new information also highlight the significance of the Sinbad Fm. for disentangling local *vs.* global signals near the late Smithian. Newly obtained age constraints and correlation also have important consequences for the understanding of the western USA basin dynamics and architecture.

1) The late middle to late Smithian age of the Sinbad Fm. in all of southwestern Utah as well as central Utah further justifies the synonymization of the Timpoweap Fm. with the Sinbad Fm.

2) The taxonomic richness of late middle Smithian assemblages is much lower in the studied area than in more northern localities. Occurrences of some taxa characteristic of the southern part of the basin, such as *Guodunites* and *Inyoites*, support the view of a spatial segregation of ammonoids within the western USA basin during the middle Smithian. However, the absence of certain middle Smithian iconic taxa, such as *Churkites* and *Meekoceras gracilitatis*, in this part of the basin is still in need of clarification. Sampled assemblages of late Smithian ammonoids include cosmopolitan taxa that are typical of this time interval worldwide and reflect the late Smithian crisis.

3) The biostratigraphical constraints obtained for the Sinbad Fm. demonstrate that the southern-most extent of the Smithian sea in the southwestern-most part of the western USA basin is further south than previously realized, reaching northern Arizona and eastern Kane County, Utah.

4) This southwestern-most excursion of the sea in the western USA basin belongs to the third order Smithian transgression-regression cycle, which is well-documented worldwide.

5) Within the studied area, the Sinbad Fm. spans the late middle to early late Smithian (*Inyoites* horizon – *Anasibirites* beds), representing presumably a short time interval, probably less than 100 kyr based on present-day estimates of Smithian ammonoid UA zones.

6) The rapid transgression-regression cycle recorded in the Sinbad Fm. appears to be primarily linked to known concomitant global warming followed by cooling changes, which led to the late Smithian extinction and to the more endemic ammonoid assemblages of the early Spathian.

7. Systematic paleontology

Systematic descriptions mainly follow the classification of Tozer (1981), and that further refined by Brayard et al. (2013), Jattiot et al. (2016, 2017) and Jenks and Brayard (2018). Quantitative morphological ranges for identified species are illustrated by scatter diagrams based on classical measurements of the diameter (D), and corresponding whorl height (H), whorl width (W) and umbilical diameter (U). Scatter diagrams of H, W and U, and H/D, W/D and U/D are provided only when the number of measured specimens is higher than four. Measurements are given in **Supplementary Table A**. The number of sampled specimens (fragmentary to complete) for each taxon and locality is indicated as "n=". Repository of figured specimens is abbreviated UBGD (Université de Bourgogne, Géologie Dijon). WW: Workman Wash; HT: Honeymoon Trail; RC: Rock Canyon; WSW: White Sage Wash.

Order Ammonoidea Zittel, 1884

Suborder Ceratitina Hyatt, 1884

Superfamily Meekoceratoidea Waagen, 1895

Family Proptychitidae Waagen, 1895

Genus ***Guodunites*** Brayard and Bucher, 2008

Type species: *Guodunites monneti* Brayard and Bucher, 2008

Guodunites hooveri (Hyatt and Smith, 1905)

Figs. 5A-M

1905 *Aspidites hooveri* Hyatt and Smith, p. 153, pl. 17, figs. 1–12.

1932 *Clypeoceras hooveri* – Smith, p. 63, pl. 17, figs. 1–12.

v 2009b *Guodunites hooveri* – Brayard et al., p. 476, pl. 2, figs. 1–30.

2010 ?*Clypeoceras hooveri* – Stephen et al., figs. 6e, f, i.

v 2013 *Guodunites hooveri* – Brayard et al., p. 170.

v 2017 *Guodunites hooveri* – Jattiot and Bucher in Jattiot et al., p. 18, pl. 4., figs. L-V.

Occurrence: Documented from the basal microbially-dominated part of the Sinbad Fm. in HT, RC (ROC2-A; n = 18) and WSW (WSW 1, WSW 2, WSW 3; n = 19). Apparently absent from WW.

Description: For thorough description and illustration of this classical middle Smithian species in the western USA basin, readers are invited to consult Brayard et al. (2009b, 2013). This taxon can be easily recognized by the main following diagnostic features: a platyconic shell with an involute coiling and a narrowly rounded venter, slightly convex flanks with maximum thickness near mid-flanks, an egressive coiling at submature stage, a deep crateriform umbilicus, and marked, projected lirae on outer shell (Brayard et al., 2009b,

2013). Weak folds are sometimes visible on the specimens presented here, but no delicate strigation as in some specimens from other sites (e.g., Brayard et al., 2009b). Suture line typically subammonitic with crenulated saddles, but only the overall architecture can be seen on our recrystallized specimens.

Measurements: See **Supplementary Fig. A** and **Supplementary Table A**. Estimated maximal size: ~15 cm (Brayard et al., 2009b, 2013).

Discussion: *Guodunites hooveri* can be distinguished from *G. monneti*, by its deeper umbilicus and its more involute coiling. Until this study, the latter had not been found in central and southern Utah suggesting a strong exclusion of these two species within the western USA basin as shown for several ammonoid taxa by Jattiot et al. (2018). However, three specimens sampled from Rock Canyon and White Sage Wash (**Fig. 5N-P**) show a rather more evolute coiling and more compressed whorl section than typical *G. hooveri* specimens, and thus are likely *G. monneti* (see next section). Both *Guodunites* species are characteristic of the middle Smithian, *G. monneti* being more cosmopolitan than *G. hooveri*, which is restricted to the western USA basin (Brayard et al., 2009b, 2013; Jattiot et al., 2017).

Guodunites monneti Brayard and Bucher, 2008

Figs. 5N-P

See Jattiot et al. (2017) and Jenks and Brayard (2018) for updated synonymy lists for this species.

Occurrence: Two specimens sampled from bed ROC2-A and one from bed WSW3 in the microbially-dominated part of the Sinbad Fm. Not yet found in other studied sections.

Description: Large sized, compressed specimens represented by an internal mold showing a moderately involute coiling and a narrowly rounded venter. Umbilicus shallow with an egressive coiling. Preserved ornamentation consists only of weak, probable lirae, visible on the umbilical margin and barely perceptible on flanks. The suture line of our specimens is poorly preserved and only shows high saddles and indented lobes. Its overall structure fits with suture lines illustrated by e.g., Brayard et al. (2009).

Measurements: See **Supplementary Table A**.

Discussion: These rare specimens mainly differ from other sampled *Guodunites* specimens by their less crateriform umbilicus and slightly more evolute coiling, thus corresponding to *G. monneti*. This species has not yet been reported from central and southern Utah.

Family Inyoitidae Spath, 1934

Genus ***Inyoites*** Hyatt and Smith, 1905

Type species: *Inyoites oweni* Hyatt and Smith, 1905

Inyoites oweni Hyatt and Smith, 1905

1905 *Inyoites oweni* Hyatt and Smith, p. 134, pl. 6, figs. 1-16; pl. 69, figs. 1-9; pl. 78, figs., 1-8.

1932 *Inyoites oweni* – Smith, p. 80, pl. 6, figs. 1-16, pl. 40, figs. 1-8, pl.69, figs. 1-9.

1934 *Inyoites oweni* – Spath, p. 138, fig. 37.

1968 *Inyoites spicini* Zakharov, p. 151, pl. 30, fig. 2.

1973 *Inyoites oweni* – Collignon, p. 12, pl.1, fig. 9.

? 1995 *Inyoites oweni* – Shevyrev, p. 34, pl. 3, figs 2-4.

2010 *Inyoites oweni* – Stephen et al., figs. 5a, b.

v 2012a *Inyoites oweni* – Brühwiler et al., p. 34, pl. 21, figs. 1-6.

? 2012a *Inyoites* sp. indet. Brühwiler et al., p. 35, pl. 21, figs. 8a-c.

v 2013 *Inyoites oweni* – Brayard et al., p. 185, fig. 49a-t.

v 2017 *Inyoites oweni* – Jattiot and Bucher in Jattiot et al., p. 24, pl. 8, figs. A-G.

v 2018 *Inyoites oweni* – Jenks and Brayard, p. 56, figs. 54q-t.

Occurrence: A unique specimen documented (but not sampled) from the microbially-dominated part of the Sinbad Fm. in HT. Not yet found in the other studied sections.

Description: See Brayard et al. (2013), Jattiot et al. (2017) and Jenks and Brayard (2018) for a thorough description and illustration of this typical late middle Smithian species in the western and southern parts of the western USA basin. Main diagnostic features include (*i*) a moderately involute and highly compressed shell bearing a characteristic high, pronounced keel, (*ii*) a shallow umbilicus, (*iii*) very conspicuous slightly sinuous fold-like ribs varying greatly in strength and width, and (*iv*) ribs rapidly fade away on the outer half of the flanks where they are gradually transformed into delicate, dense and sinuous lirae. Suture line not visible on our specimen.

Measurements: Estimated maximal size: ~8 cm (Brayard et al., 2013).

Discussion: Two additional *Inyoites* species (*I. beaverensis* and *I. stokesi*) are known from the Smithian of the western USA basin (Brayard et al., 2013; Jenks and Brayard, 2018). *Inyoites beaverensis* is older (early middle Smithian) and mainly differs from the type species by its more evolute coiling, its near-absence of ornamentation and its smaller keel (Brayard et al., 2013; Jattiot et al., 2017). Intermediate forms between *I. beaverensis* and *I. oweni* were also reported from the late middle Smithian of Nevada (Jattiot et al., 2017). *Inyoites stokesi* co-occurs with *I. oweni*, but differs by its barely perceptible keel as well as its slightly more involute coiling. *Inyoites oweni* is typical of the late middle Smithian in the western USA basin and facilitates correlation worldwide (e.g., with the *Inyoites* horizon of the *Owenites* beds in South China; see Brayard and Bucher, 2008).

Family Prionitidae Hyatt, 1900

Genus ***Gurleyites*** Mathews, 1929

Type species: *Gurleyites smithi* Mathews, 1929

Gurleyites smithi Mathews, 1929

Figs. 6A-Q, 7A-S, 8A-O, 9A-J, 10A-H

? 1929 *Goniodiscus ornatus* Mathews, p. 34, pl. 6, figs. 6-10.

? 1929 *Goniodiscus* (?) *varians* Mathews, p. 35, pl. 7, figs. 26-39.

1929 *Kashmirites resseri* Mathews, p. 38, pl. 8, figs. 4-7.

? 1929 *Anasibirites edsoni* Mathews, p.27, pl. 4, figs. 29-32

? 1929 *Anasibirites bassleri* Mathews, p.28, pl. 4, figs. 33-35

? 1929 *Anasibirites mojsisovicsi* Mathews, p. 30, pl. 5, figs. 1-3

1929 *Gurleyites smithi* Mathews, p. 43, pl. 10, figs. 1-6.

1929 *Gurleyites bastini* Mathews, p. 44, pl. 10, figs. 7-11.

p 1929 *Gurleyites chamberlini* Mathews, p. 44, pl. 11, figs. 3-5.

1929 *Gurleyites milleri* Mathews, p. 45, pl. 9, figs. 10-12.

1929 *Gurleyites boutwelli* Mathews, p. 45, pl. 8, figs. 1-3.

1932 *Kashmirites resseri* – Smith, p. 67, pl. 81, figs. 9, 10.

? 1932 *Anasibirites mojsisovicsi* – Smith, p. 73, pl. 80, figs. 1-2.

1932 *Anasibirites bastini* – Smith, p. 70, pl. 80, figs. 3-5.

? 1932 *Anasibirites ornatus* – Smith, p. 75, pl. 80, figs. 11, 12.

1932 *Anasibirites smithi* – Smith, p. 76, pl. 80, figs. 13-15.

1961 *Arctoprionites* sp. indet. Tozer, pl. 20, figs. 1, 3.

v 1962 *Arctoprionites* sp. indet. Kummel and Steele, p. 699, pl. 101, fig. 2.

? 1976 *Gurleyites debilis* Wang and He, p. 296, pl. 7, figs. 23-24.

1994 *Arctoprionites williamsi* Tozer, p. 83, pl. 34, figs. 1-4.

v 2013 *Anasibirites* cf. *angulosus* – Brayard et al., p. 195, fig. 65.

v 2013 *Arctoprionites resseri* – Brayard et al., p. 198, fig. 67.

2015 *Arctoprionites resseri* – Piazza, p. 52, pl. 2, figs. e-g.

v 2017 *Arctoprionites resseri* – Jattiot and Bucher in Jattiot et al., p. 34, pl. 12, figs. N-X.

2017 *Arctoprionites resseri* – Piazza in Piazza et al., fig. 4C-D.

p v 2018 *Hemiprionites typus* – Jenks and Brayard, figs. 78D-F, 79G-I only.

v 2018 *Arctoprionites resseri* – Jenks and Brayard, p. 92, fig. 86-87.

2020 *Arctoprionites resseri* – Jattiot et al., p. 55, pl. 28P-U.

Occurrence: Abundant in the microbially-dominated unit of the Sinbad Fm. in WW (BRC; n = 85).

Description: Compressed and moderately involute prionitid showing a slightly egressive coiling, and a sulcate to delicately arched venter, many specimens exhibiting a tabulate venter. Ornamentation is characteristically highly variable among specimens and sometimes throughout ontogeny. It generally consists of forward projected, bullate, elongated and sinuous ribs that stem near the umbilical shoulder and fade rapidly toward the venter (see also description of "*Arctoprionites resseri"* in Brayard et al., 2013; Jattiot et al., 2017; Jenks and Brayard, 2018). The newly sampled, well-preserved specimens from Workman Wash indicate that these ribs may cross the venter, resulting in a slightly crenulated venter. Some rare specimens also exhibit elevated bullate ribs that almost form tubercles in a manner similar to *Wasatchites*. Specimens with a more evolute coiling generally exhibit a stronger ornamentation, thereby complying with Buckman's rules of covariation (Westermann, 1966; Monnet et al., 2015). Umbilical margin is broadly arched with an inclined wall.

As a complement to previous works, our abundant and well-preserved material shows a feature not previously reported for this taxon, which consists of a strigation on the venter and on the flanks, most often on both sides of the ventrolateral margin. These spiral lines can be seen at all growth stages, but often do not continue throughout the entire ontogeny. Additionally, they are more or less well expressed and are apparently independent from the venter shape. This strigation may also occur asymmetrically on the venter of some specimens and more rarely, may shift a little further towards the internal part of the flank. One specimen also exhibits on its inner whorls, regularly spaced relief that strongly resembles megastriae (**Fig. 9I-J**). The suture line is rarely observable on our specimens and is often incomplete. However, it is typical of the genus with three large, arched saddles, decreasing in size from the ventrolateral to the umbilical margin. Lobes are well indented.

Measurements: See **Supplementary Fig. B** and **Supplementary Table A**. Estimated maximal size: ~15 cm (Jenks and Brayard, 2018).

Discussion: The genus *Gurleyites* is a typical example of the complicated taxonomy of prionitids as members of this family show a marked intraspecific variation. The newly sampled material leads us to merge all *Gurleyites* species and two *Goniodiscus* species erected by Mathews (1929) with the more recent taxon *Arctoprionites* erected by Spath (1930), including specimens described as *Kashmirites resseri* by Mathews (1929), as well as all Mathews' specimens that fit well within the now known much wider intraspecific variation of *Gurleyites smithi*. Since *G. smithi* is the type species of *Gurleyites* and has priority, *Arctoprionites resseri* is now considered to be a junior synonym. Jattiot et al. (2016) tentatively synonymized some *Gurleyites* species with *A. kingianus*. This similarity was also discussed by Spath (1934) who highlighted the existence of a few intermediate juvenile forms between e.g., *Anasibirites* and *Gurleyites*, and by Tozer (1971) who synonymized *Gurleyites* with *Anasibirites.* In 1930, Spath erected the new genus *Arctoprionites* for *Goniodiscus nodosus* from Spitsbergen (Frebold, 1930), which also served as a new genus name for specimens of "*Kashmirites resseri*" from the western USA basin. *Arctoprionites nodosus* closely resembles *Gurleyites smithi* (see Jenks and Brayard, 2018 for explanations on potential differences between these two species). Even though we consider *A. nodosus* to be a possible valid species, typical of the Boreal late Smithian, it is extremely difficult to justify why it also should not be placed within the genus *Gurleyites*. Spath (1934) erected three additional prionitid taxa from Spitsbergen, i.e., *Gurleyites freboldi, Hemiprionites gardwoodi* and *Arctoprionites tyrrelli*, which are very close to *A. nodosus* and actually are probably variants of this species. In terms of whorl shape and coiling geometry, these four taxa are practically indistinguishable from *Gurleyites smithi* (compare our **Supplementary Material**

Fig. B and measurements of *A. nodosus* provided by Piazza, 2015), the only difference being slight but apparently consistent differences in ornamentation (e.g., shape and trajectory of ribs, and nodes on the flanks of *A. nodosus* appear to be placed farther toward the venter than on *Gurleyites smithi*). These ornamental variances can justify a separate species, but probably not a separate genus. Therefore, we place *A. nodosus* within *Gurleyites* and invalidate the genus *Arctoprionites*.

Gurleyites smithi shows a rather large geographic distribution as do most early late Smithian prionitid genera, (e.g., Spitsbergen: Frebold, 1930, Piazza et al., 2017; British Columbia: Tozer, 1994; Timor: Jattiot et al., 2020). It is found at several places in the eastern and southern parts of the western USA basin, but is often rare (Brayard et al., 2013; Jattiot et al., 2017; Jenks and Brayard, 2018). However, this is not the case at Workman Wash, where the taxon occurs abundantly.

The newly sampled material also leads us to reassign certain specimens attributed to *H. typus* by Jenks and Brayard (2018; figs. 78D-G, 79G-I) to *Gurleyites smithi* (note that these specimens show a very weak ventral strigation; see implications hereafter). In addition, it leads us to integrate specimens of *Anasibirites* cf. *angulosus* illustrated by Brayard et al. (2013) into *G. smithi*. *Gurleyites debilis*, erected by Wang and He (1976) for prionitid specimens from southern Tibet, may fit within *G. smithi*. However, the poor preservation and inadequate illustration of these specimens prevent a firm assignment. Specimens assigned to *Gurleyites* and *Arctoprionites* have also been reported from South Primorye (e.g., Zakharov, 1978), but detailed comparisons based on more illustrated material are needed before these assignments can be validated.

The observed spiral lines on the venter and on the flanks are a newly observed ornamental feature indicating that *Gurleyites*, similar to another Prionitidae, *Hemiprionites* (e.g., Jattiot et al., 2017; Jenks and Brayard, 2018), exhibits strigation on well-preserved specimens.

Although strigation has occasionally been documented and illustrated for *Hemiprionites*, this feature has rarely been integrated into taxonomic descriptions and discussed. This also indicates that, like many other Smithian families (e.g., Flemingitidae, Arctoceratidae, Proptychitidae), the Prionitidae include at least two representatives that exhibit strigation, and that this ornamentation is therefore common among Smithian ammonoids.

Newly sampled specimens of *Gurleyites smithi* illustrate that this species exhibits a very large intraspecific variation. Notably, it overlaps the intraspecific variation of *Hemiprionites typus.* Specimens of *G. smithi* exhibiting weak ornamentation may indeed be confused with some "robust" specimens of *H. typus*, which may bear highly sinuous, bullate folds and ventral strigation. However, in contrast with *G. smithi, H. typus* specimens apparently do not exhibit a prominent relief near the umbilical margin and sometimes bear a minute depression just below the ventral shoulder (see Jattiot et al., 2017 and Jenks and Brayard, 2018 for a discussion on the diagnostic nature of the latter's ornamentation). Some large specimens of *G. smithi* may also display later growth stages that resemble those of *H. typus* (**Fig. 8L-O**). Some workers may therefore see a morphological continuum between these two taxa. Based on this and other recent studies, this indicates that they, at the very least, are very closely-related prionitid species. *G. smithi* specimens are on average slightly more evolute than typical *H. typus* (**Supplementary Fig. C**), but this observation is highly dependent on the robustness of their ornamentation. Additionally, some rare specimens of *G. smithi* have elevated bullate ribs that may almost form tubercles (**Fig. 8A-C, F-H**). Such specimens can thus be confused with poorly preserved *Wasatchites* specimens. However, they differ by their highly variable ornamentation throughout ontogeny; this ornamentation is generally weaker than that of *Wasatchites*. Nevertheless, these specimens suggest a rather close phylogenetic affinity between *Gurleyites* and *Wasatchites*. Finally, one specimen also bears megastriae on its inner whorls (**Fig. 9I-J**); this feature is remindful of the megastriae observed in *Anasibirites*

721 species, thus also supporting a possible close phylogenetic link between *Anasibirites* and
722 *Gurleyites*. This resemblance between both genera, found in a few *Gurleyites* specimens, was
723 earlier noticed by Spath (1934).
724 The suture line of *G. smithi* and its variability have rarely been well illustrated. The overall
725 architecture of the suture line observed on our specimens fits well with those documented
726 from specimens sampled at Palomino Ridge and Crittenden Springs, Nevada, and illustrated
727 by Jattiot et al. (2017) and Jenks and Brayard (2008), respectively. This observation suggests
728 that the intraspecific variability of the suture line is somewhat restricted for this species. By
729 contrast, saddles of *H. typus* appear more pinched and its first lateral saddle more flared (see
730 also Jenks and Brayard, 2018 for comparison). However, the number of suture lines illustrated
731 for *H. typus* is still rather restricted, thus preventing a precise assessment of its intraspecific
732 variability.
733
734 Genus ***Wasatchites*** Mathews, 1929
735 **Type species**: *Wasatchites perrini* Mathews, 1929
736
737 *Wasatchites perrini* Mathews, 1929
738 **Figs. 9K-L**
739
740 1929 *Wasatchites perrini* Mathews, p. 40, pl. 9, figs. 1–9
741 1929 *Wasatchites meeki* Mathews, p. 41, pl. 7, figs. 1–3; pl. 8, figs. 11–14.
742 1929 *Wasatchites magnus* Mathews, p. 41, pl. 11, figs. 1, 2.
743 1929 *Wasatchites quadratus* Mathews, p. 42, pl. 7, figs. 23–25.
744 ? 1929 *Kashmirites thornei* Mathews, p. 38, pl. 6, figs. 22–25.
745 1929 *Kashmirites wasatchensis* Mathews, p. 36, pl. 6, figs. 26–28.

? 1929 *Kashmirites gilberti* Mathews, p. 38, pl. 7, figs. 4–8.

1929 *Keyserlingites seerleyi* Mathews, p. 39, pl. 8, figs. 8–10.

1932 *Kashmirites meeki* – Smith, p. 67, pl. 81, figs. 1, 2.

1932 *Kashmirites wasatchensis* Smith, p. 69, pl. 81, figs. 3–5.

1932 *Kashmirites perrini* – Smith, p. 67, pl. 81, figs. 6–8.

1932 *Kashmirites seerleyi* Smith, p. 68, pl. 81, figs. 11, 12.

p 1961 *Wasatchites tardus* Tozer, p. 71, pl. 19, figs. 1a-b (only).

1994 *Wasatchites perrini* – Tozer, p. 79, pl. 29, figs. 5a-c; pl. 35, figs. 2-4.

v 2010 *Wasatchites perrini* – Stephen et al., fig. 7c.

v 2013 *Wasatchites perrini* – Brayard et al., p. 191, figs. 13d, 59a-k.

v 2017 *Wasatchites perrini* – Jattiot and Bucher in Jattiot et al., p. 28, figs. 13d, 59a-k.

v 2018 *Wasatchites perrini* – Jenks and Brayard, p. 87, fig. 83.

Occurrence: Documented from the microbially-dominated unit of the Sinbad Fm. in WW (BRC; n = 2) and its upper part in RC (ROC3-A; not sampled).

Description: Reader should refer to Brayard et al. (2013), Jattiot et al. (2017) and Jenks and Brayard (2018) for detailed descriptions and discussions of this typical early late Smithian taxon. This species exhibits a rather large intraspecific variation, but the shell is generally moderately involute with a trapezoidal whorl section. Its ornamentation consists of (*i*) very conspicuous tubercles on umbilical shoulders that become more bullate or nodate on mature whorls, but then tend to rapidly lose strength near the aperture, and (*ii*) alternating strong and weak, fasciculate ribs that stem from the tubercles and cross the venter. The venter is also subtabulate to slightly arched. Suture line unknown from the studied specimens.

Measurements: Sampled specimens are all fragmented, preventing measurements. Estimated maximal size: ~20 cm (Jenks and Brayard, 2018).

Discussion: *W. perrini* can be distinguished from other co-occurring taxa by its conspicuous, regularly spaced ornamentation. This species is not very abundant in the western USA basin compared to, e.g., *Anasibirites*. A second species of *Wasatchites* (*W.* cf. *distractus*) has been reported from the early late Smithian at one locality within the western USA basin, i.e., Crittenden Springs, Nevada (Jenks and Brayard, 2018). This species, previously known only from the Tethys (e.g., Brühwiler et al., 2012b, c), mainly differs from the type species by its more broadly rounded venter at all growth stages, the mid-flank position of its tubercles, and its more radially directed ribs. *Wasatchites* is an emblematic early late Smithian prionitid that shows a large cosmopolitan distribution (e.g., Brayard et al., 2006). It is thus a helpful taxon that can be used as an auxiliary marker to *Anasibirites* to delineate the early late Smithian worldwide.

Genus ***Anasibirites*** Mojsisovics, 1896

Type species: *Sibirites kingianus* Waagen, 1895

Remark: Jattiot et al. (2016) provided a comprehensive review of the taxonomy of the various iconic late Smithian *Anasibirites* species. We follow the conclusions of this work and thus do not include the complete description and synonymy list for each sampled species. Reader should refer to Jattiot et al. (2016) for complete synonymy lists (see also our remarks on species included in *G. smithi*).

Anasibirites multiformis Welter, 1922

Fig. 11A-P

v 2016 *Anasibirites multiformis* – Jattiot et al., p. 184, figs. 10N–S, 21–23 [cum syn.].

v 2017 *Anasibirites multiformis* – Jattiot and Bucher in Jattiot et al., p. 30, pl. 11, figs. G-AA.

v 2018 *Anasibirites multiformis* – Jenks and Brayard, p. 79, figs. 74D-F, G(4,5), 75.

Occurrence: Documented from the microbially-dominated unit of the Sinbad Fm. in WW (BRC; n = 28) and its upper part in RC (ROC3-A; n = 2).

Description: Rather involute, compressed prionitid with near isometric growth. Ornamentation typically consists of weak and dense megastriae throughout ontogeny. Suture line unknown for sampled specimens.

Measurements: See **Supplementary Fig. D** and **Supplementary Table A**. Estimated maximal size: ~10 cm (Jattiot et al., 2016).

Discussion: This species is abundant within the studied area, but is mainly represented by small-sized specimens, generally < 4 cm (**Fig. 11**). As shown by Jattiot et al. (2016), the occurrence of megastriae mimicking the intercalation of strong ribs only on the inner whorls (often <20 mm) is essential for distinguishing *A. kingianus* from *A. multiformis.* The latter display weaker and denser megastriae throughout ontogeny. *A. multiformis* is also less variable with a generally more compressed whorl and near isometric growth. *A. multiformis* is much more abundant than *A. kingianus* in the western USA basin (Jattiot et al., 2016; Jenks and Brayard, 2018). *Anasibirites* is an iconic genus utilized worldwide to define the base of the late Smithian (e.g., Brühwiler et al., 2010), as it shows a highly cosmopolitan distribution

821 that includes Siberia, Spitsbergen, British Columbia, western USA, Timor, Spiti, Salt Range,
822 Kashmir, Afghanistan, South China, Oman, South Primorye and Japan (e.g., Jattiot et al.,
823 2016).
824
825 Genus ***Hemiprionites*** Spath, 1929
826 **Type species:** *Goniodiscus typus* Waagen, 1895
827
828 *Hemiprionites typus* (Waagen, 1895)
829 **Figs. 10A-H, 12J-S**
830
831 1895 *Goniodiscus typus* Waagen, p. 128, pl. 9, figs. 7-10.
832 1929 *Goniodiscus typus* – Mathews, p. 31, pl. 5, figs. 12-21.
833 1929 *Goniodiscus americanus* – Mathews, p. 32, pl. 5, figs. 22-27.
834 1929 *Goniodiscus shumardi* – Mathews, p. 33, pl. 6, figs. 11-14.
835 1929 *Goniodiscus utahensis* – Mathews, p. 33, pl. 6, figs. 29-31.
836 1929 *Goniodiscus slocomi* – Mathews, p. 34, pl. 6, figs. 15-17.
837 1929 *Goniodiscus butleri* – Mathews, p. 35, pl. 6, figs. 18-21.
838 1932 *Anasibirites typus* – Smith, p. 76, pl. 80, figs. 6-8.
839 1932 *Anasibirites utahensis* – Smith, p. 77, pl. 80, figs. 9, 10.
840 1934 *Hemiprionites typus* – Spath, p. 331, figs. 114ac.
841 v p 2008 *Hemiprionites* cf. *H. butleri* – Brayard and Bucher, p. 58, pl. 29, figs 1, 4, 7 only,
842 text- fig. 50.
843 2012b *Hemiprionites typus* – Brühwiler and Bucher, p. 103, figs. 89A-AH.
844 v 2013 *Hemiprionites* cf. *H. typus* – Brayard et al., p. 197, fig. 66.

v 2017 *Hemiprionites typus* – Jattiot and Bucher in Jattiot et al., p. 31, pl. 12, figs. A-M, pl. 13, figs. A-X.

p v 2018 *Hemiprionites typus* – Jenks and Brayard, p. 81, figs. 77, 78A-C, 78G-R, 79A-F,.79J-O.

2020 *Hemiprionites typus* – Jattiot et al., p. 56, pl. 29A-AN.

Occurrence: Documented from the microbially-dominated unit of the Sinbad Fm. in WW (BRC; n = 20).

Description: See taxonomic revision of *Hemiprionites* species by Jattiot et al. (2017). The type species shows a compressed shell with variable involution and a typical marked egressive coiling at mature stage. A small depression on the outer edge of the flank, just below the ventral margin, is also visible on some specimens (e.g., **Fig. 12N**). Spiral lines are sometimes visible on the venter and/or near the ventrolateral margin (e.g., **Figs. 12K, R-S**). Flexuous and slightly biconcave growth lines are visible and may bundle into small folds that may cross the venter. Suture line ceratitic with a deep and flared first lateral lobe. Saddles appear pinched.

Measurements: See **Supplementary Fig. E** and **Supplementary Table A**. Estimated maximal size: ~10 cm (Jattiot et al., 2017).

Discussion: *H. typus* is a characteristic early late Smithian taxon. It can be distinguished from another co-occurring *Hemiprionites* species, *H. walcotti*, by its often wider venter and umbilicus, as well as by more egressive coiling and the existence of a small depression near the ventral margin on some specimens. Another *Hemiprionites* species, *H. roberti*, is

documented from the western USA basin but is late middle Smithian in age (Jenks et al., 2010). *H. roberti* does not exhibit egressive coiling and has a funnel-shaped umbilicus. The morphological variability of *H. typus* partly overlaps with *Gurleyites smithi*, but the latter appears more ornamented and slightly more evolute, and has a somewhat different suture line (see *G. smithi* discussion).

Hemiprionites walcotti (Mathews, 1929)

Fig. 12A-I

p 1922 *Anasibirites multiformis* Welter, p. 17, figs. 4-7, 11-14.

1929 *Goniodiscus walcotti* Mathews, p. 32, pl. 6, figs. 1-5.

1934 *Hemiprionites timorensis* Spath, p. 331.

v p 2008 *Hemiprionites* cf. *H. butleri* – Brayard and Bucher, p. 58, pl. 29, figs. 2, 3, 6 only.

v 2008 *Hemiprionites klugi* Brayard and Bucher, p. 59, pl. 30, figs. 1-4.

p 2012a *Hemiprionites* cf. *H. butleri* – Brühwiler and Bucher, p. 33, pl. 19, figs. 10 only.

p 2012b *Anasibirites angulosus* – Brühwiler and Bucher, p. 103, figs. 87H-J, N-P only.

2012b *Hemiprionites klugi* – Brühwiler and Bucher, p. 103, figs. 87Q-AB.

v 2017 *Hemiprionites walcotti* – Jattiot and Bucher in Jattiot et al., p. 34, pl. 14, figs. A-Y.

v 2018 *Hemiprionites walcotti* – Jenks and Brayard, p. 83, figs. 79Q-V.

2020 *Hemiprionites walcotti* – Jattiot et al., p. 57, pl. 29AT-BG.

Occurrence: Documented from the microbially-dominated unit of the Sinbad Fm. in WW (BRC; n = 5).

Description: See taxonomic revision of *Hemiprionites* species by Jattiot et al. (2017). This species exhibits a more involute and less egressive coiling than the type species. The umbilicus is deep with a steeply inclined wall. Radial folds are sometimes visible together with flexuous growth lines following the trajectory of the folds. Suture line unknown for sampled specimens.

Measurements: See **Supplementary Fig. F** and **Supplementary Table A**. Estimated maximal size: ~7 cm (Jattiot et al., 2017).

Discussion: See *H. typus* discussion.

Declaration of Competing Interests

Authors have no competing interests to declare.

Acknowledgements

This work is a contribution to the ANR project AFTER (ANR-13-JS06-0001-01) and was also supported by the French "Investissements d'Avenir" program, project ISITE-BFC (ANR-15-IDEX-03). The final version of this paper benefited from constructive reviews by Spencer Lucas and two anonymous referees. S. Ritter (BYU) shared some locality data (HT). We thank G. Caravaca, T. Hurd and P. Guenser for their help in the field. The studied sections are located on US public land under the stewardship of the Bureau of Land Management (BLM) of the US Department of the Interior; access to these lands is gratefully acknowledged.

References

Bagherpour, B., Bucher, H., Baud, A., Brosse, M., Vennemann, T., Martini, R., Guodun, K., 2017. Onset, development, and cessation of basal Early Triassic microbialites (BETM) in the Nanpanjiang pull-apart Basin, South China Block. Gondwana Research 44, 178-204. https://doi.org/10.1016/j.gr.2016.11.013.

Baresel, B., Bucher, H., Brosse, M., Cordey, F., Guodun, K., Schaltegger, U., 2017. Precise age for the Permian–Triassic boundary in South China from high-precision U-Pb geochronology and Bayesian age–depth modeling. Solid Earth 8, 361-378. https://doi.org/10.5194/se-8-361-2017

Behrensmeyer, A.K., Kidwell, S., Gastaldo, R.A., 2000. Taphonomy and paleobiology. Paleobiology 26, 103-147.

Blakey, R.C., 1979. Oil impregnated carbonate rocks of the Timpoweap Member, Moenkopi Formation, Hurricane Cliffs area, Utah and Arizona. Utah Geology 6, 45-54.

Brayard, A., Brühwiler, T., Bucher, H., Jenks, J., 2009a. *Guodunites*, a low-palaeolatitude and trans-Panthalassic Smithian (Early Triassic) ammonoid genus. Palaeontology 52, 471-481. https://doi.org/10.1111/j.1475-4983.2009.00855.x.

Brayard, A., Bucher, H., 2008. Smithian (Early Triassic) ammonoid faunas from northwestern Guangxi (South China): taxonomy and biochronology. Fossils and Strata 55, 179 pp.

Brayard, A., Bucher, H., Escarguel, G., Fluteau, F., Bourquin, S., Galfetti, T., 2006. The Early Triassic ammonoid recovery: paleoclimatic significance of diversity gradients. Palaeogeography, Palaeoclimatology, Palaeoecology 239, 374-395. https://doi.org/10.1016/j.palaeo.2006.02.003.

Brayard, A., Bylund, K., Jenks, J., Stephen, D., Olivier, N., Escarguel, G., Fara, E., Vennin, E., 2013. Smithian ammonoid faunas from Utah: implications for Early Triassic

biostratigraphy, correlation and basinal paleogeography. Swiss Journal of Palaeontology 132, 141-219. https://doi.org/10.1007/s13358-013-0058-y.

Brayard, A., Escarguel, G., Bucher, H., 2007. The biogeography of Early Triassic ammonoid faunas: Clusters, gradients and networks. Geobios 40, 749-765. https://doi.org/10.1016/j.geobios.2007.06.002.

Brayard, A., Escarguel, G., Bucher, H., Monnet, C., Brühwiler, T., Goudemand, N., Galfetti, T., Guex, J., 2009b. Good genes and good luck: Ammonoid diversity and the end-Permian mass extinction. Science 325, 1118-1121. DOI: 10.1126/science.1174638.

Brayard, A., Krumenacker, L.J., Botting, J.P., Jenks, J.F., Bylund, K.G., Fara, E., Vennin, E., Olivier, N., Goudemand, N., Saucède, T., Charbonnier, S., Romano, C., Doguzhaeva, L., Thuy, B., Hautmann, M., Stephen, D.A., Thomazo, C., Escarguel, G., 2017. Unexpected Early Triassic marine ecosystem and the rise of the Modern evolutionary fauna. Science Advances 3, e1602159. DOI: 10.1126/sciadv.1602159.

Brayard, A., Meier, M., Escarguel, G., Fara, E., Nützel, A., Olivier, N., Bylund, K.G., Jenks, J.F., Stephen, D.A., Hautmann, M., Vennin, E., Bucher, H., 2015. Early Triassic Gulliver gastropods: Spatio-temporal distribution and significance for biotic recovery after the end-Permian mass extinction. Earth-Science Reviews 146, 31-64. https://doi.org/10.1016/j.earscirev.2015.03.005.

Brayard, A., Vennin, E., Olivier, N., Bylund, K.G., Jenks, J., Stephen, D.A., Bucher, H., Hofmann, R., Goudemand, N., Escarguel, G., 2011. Transient metazoan reefs in the aftermath of the end-Permian mass extinction. Nature Geoscience 4, 693-697. https://doi.org/10.1038/ngeo1264.

Brett, C.E., 1995. Sequence stratigraphy, biostratigraphy, and taphonomy in shallow marine environment. Palaios 10, 597-616.

967 Brosse, M., Bucher, H., Goudemand, N., 2016. Quantitative biochronology of the Permian–
968 Triassic boundary in South China based on conodont unitary associations. Earth-Science
969 Reviews 155, 153-171. https://doi.org/10.1016/j.earscirev.2016.02.003.
970 Brühwiler, T., Bucher, H., Brayard, A., Goudemand, N., 2010. High-resolution biochronology
971 and diversity dynamics of the Early Triassic ammonoid recovery: The Smithian faunas of
972 the Northern Indian Margin. Palaeogeography, Palaeoclimatology, Palaeoecology 297,
973 491-501. https://doi.org/10.1016/j.palaeo.2015.09.013.
974 Brühwiler, T., Bucher, H., Goudemand, N., Galfetti, T., 2012a. Smithian (Early Triassic)
975 ammonoid faunas from Exotic Blocks from Oman: taxonomy and biochronology.
976 Palaeontographica Abteilung A 296, 3-107. DOI: 10.1127/pala/296/2012/3.
977 Brühwiler, T., Bucher, H., Krystyn, L., 2012b. Middle and late Smithian (Early Triassic)
978 ammonoids from Spiti (India). Special Papers in Palaeontology 88, 115-174.
979 https://doi.org/10.1111/j.1475-4983.2012.01202.x
980 Brühwiler, T., Bucher, H., Ware, D., Hermann, E., Hochuli, P.A., Roohi, G., Rehman, K.,
981 Yassen, A., 2012c. Smithian (Early Triassic) ammonoids from the Salt Range. Special
982 Papers in Palaeontology 88, 1-114. https://doi.org/10.1111/j.1475-4983.2012.01204.x.
983 Caravaca, G., Brayard, A., Vennin, E., Guiraud, M., Le Pourhiet, L., Grosjean, A.-S.,
984 Thomazo, C., Olivier, N., Fara, E., Escarguel, G., Bylund, K.G., Jenks, J.F., Stephen, D.A.,
985 2018. Controlling factors for differential subsidence in the Sonoma Foreland Basin (Early
986 Triassic, western USA). Geological Magazine 155, 1305-1329.
987 doi:10.1017/S0016756817000164.
988 Caravaca, G., Thomazo, C., Vennin, E., Olivier, N., Cocquerez, T., Escarguel, G., Fara, E.,
989 Jenks, J.F., Bylund, K.G., Stephen, D.A., Brayard, A., 2017. Early Triassic fluctuations of
990 the global carbon cycle: New evidence from paired carbon isotopes in the western USA

basin. Global and Planetary Change 154, 10-22. https://doi.org/10.1016/j.gloplacha.2017.05.005.

Clark, D.L., Carr, T.R., 1984. Conodont biofacies and biostratigraphic schemes in western North America: a model, in: Clark, D.L. (Ed.), Conodont biofacies and provincialism, GSA Special Paper 196, 1-9.

Clarkson, M.O., Wood, R.A., Poulton, S.W., Richoz, S., Newton, R.J., Kasemann, S.A., Bowyer, F., Krystyn, L., 2016. Dynamic anoxic ferruginous conditions during the end-Permian mass extinction and recovery. Nature Communication 7, 12236. https://doi.org/10.1038/ncomms12236.

Collinson, J.W., Kendall, C.G.S.C., Marcantel, J.B., 1976. Permian-Triassic boundary in eastern Nevada and west-central Utah. Bulletin of the Geological Society of America 87, 821-824.

Collinson, J.W., Hasenmueller, W.A., 1978. Early Triassic paleogeography and biostratigraphy of the Cordilleran miogeosyncline, in: Reynolds, M.W., Dolly, E.D. (Eds.), Mesozoic paleogeography of the western United States. Society of Economic Paleontologists and Mineralogists, Pacific Section, pp. 175-186.

Dagys, A.S., 1988. Major features of the geographic differentiation of Triassic ammonoids (eds Wiedmann, J., Kullmann, J.), pp. 341-349, Cephalopods - Present and Past. Schweizerbart'sche Verlagsbuchhandlung, Stuttgart.

Dickinson, W.R., 2013. Phanerozoic palinspastic reconstructions of Great Basin geotectonics (Nevada-Utah, USA). Geosphere 9, 1384-96. https://doi.org/10.1130/GES00888.1.

Doelling, H.H., Davis, F.D., 1989. The geology of Kane County, Utah. Utah Geological and Mineral Survey 124, 1-192.

Embry, A.F., 1988. Triassic sea-level changes: evidence from the Canadian Artic archipelago. Sea-level changes-An integrated approach, SEPM Special Publication 42, 249-259.

1016 Embry, A.F., 1997. Global sequence boundaries of the Triassic and their identification in the
1017 Western Canada sedimentary basin. Bulletin of Canadian Petroleum Geology 45, 415-433.
1018 Frebold, H., 1930. Die altersstellung des fischhorizontes, des grippianiveaus und des unteren
1019 saurierhorizontes in Spitzbergen. Skrifter om Svalbard og Ishavet 28, 1-36.
1020 Galfetti, T., Bucher, H., Ovtcharova, M., Schaltegger, U., Brayard, A., Brühwiler, T.,
1021 Goudemand, N., Weissert, H., Hochuli, P.A., Cordey, F., Guodun, K.A., 2007. Timing of
1022 the Early Triassic carbon cycle perturbations inferred from new U-Pb ages and ammonoid
1023 biochronozones. Earth and Planetary Science Letters 258, 593-604.
1024 https://doi.org/10.1016/j.epsl.2007.04.023.
1025 Goodspeed, T.H., Lucas, S.G., 2007. Stratigraphy, sedimentology, and sequence stratigraphy
1026 of the Lower Triassic Sinbad Formation, San Rafael Swell, Utah. New Mexico Museum of
1027 Natural History and Science Bulletin 40, 91-101.
1028 Gornitz, V., Lebedeff, S., Hansen, J., 1982. Global sea level trend in the past century. Science
1029 215, 1611-1614. https://doi.org/10.1126/science.215.4540.1611.
1030 Goudemand, N., Romano, C., Leu, M., Bucher, H., Trotter, J.A., Williams, I.S., 2019.
1031 Dynamic interplay between climate and marine biodiversity upheavals during the early
1032 Triassic Smithian -Spathian biotic crisis. Earth-Science Reviews 195, 169-178.
1033 https://doi.org/10.1016/j.earscirev.2019.01.013
1034 Grasby, S.E., Beauchamp, B., Embry, A., Sanei, H., 2013. Recurrent Early Triassic ocean
1035 anoxia. Geology 41, 175-178. https://doi.org/10.1130/G33599.1.
1036 Gregory, H.E., 1948. Geology and geography of Central Kane County, Utah. GSA Bulletin
1037 59, 211-248.
1038 Gregory, H.E., 1950. Geology and geography of the Zion National Park region, Utah and
1039 Arizona. US Geological Survey Professional Paper 220, 1-200.

1040 Hallam, A., 1996. Major bio-events in the Triassic and Jurassic, in: Walliser, O.H. (Ed.)
1041 Global Events and Event stratigraphy in the Phanerozoic: results of the International
1042 Interdisciplinary Cooperation in the IGCP-Project 216 "Global Biological Events in Earth
1043 History", Springer-Verlag, pp. 265-283.
1044 Haq, B.U., 2018. Triassic eustatic variations reexamined. GSA Today 28, 4-9. DOI:
1045 10.1130/GSATG381A.1.
1046 Haq, B.U., Al-Qahtani, A.M., 2018. Phanerozoic cycles of sea-level change on the Arabian
1047 Platform. GeoArabia 10, 127-160.
1048 Hautmann, M., Smith, A.B., McGowan, A.J., Bucher, H., 2013. Bivalves from the Olenekian
1049 (Early Triassic) of south-western Utah: systematics and evolutionary significance. Journal
1050 of Systematic Palaeontology 11, 263-293. https://doi.org/10.1080/14772019.2011.637516.
1051 Hay, W.W., Leslie, M.A., 1990. Could possible changes in global groundwater reservoir
1052 cause eustatic sea level fluctuations?, Geophysics Study Committee, Mathematics and
1053 Resources, National Research Council (Eds.), Sea Level Change: Studies in Geophysics,
1054 National Academy Press, Washington D.C., pp. 161-170.
1055 Hermann, E., Hochuli, P.A., Bucher, H., Roohi, G., 2012. Uppermost Permian to Middle
1056 Triassic palynology of the Salt Range and Surghar Range, Pakistan. Review of
1057 Palaeobotany and Palynology 169, 61-95. https://doi.org/10.1016/j.revpalbo.2011.10.004.
1058 Hochuli, P.A., Vigran, J.O., 2010. Climate variations in the Boreal Triassic - Inferred from
1059 palynological records from the Barents Sea. Palaeogeography, Palaeoclimatology,
1060 Palaeoecology 290, 20-42. https://doi.org/10.1016/j.palaeo.2009.08.013.
1061 Hofmann, R., Hautmann, M., Bucher, H., 2017. Diversity partitioning in Permian and Early
1062 Triassic benthic ecosystems of the Western USA: a comparison. Historical Biology 29,
1063 918-930. https://doi.org/10.1080/08912963.2016.1263626.

1064 Hofmann, R., Hautmann, M., Wasmer, M., Bucher, H., 2013. Palaeoecology of the Spathian
1065 Virgin Formation (Utah, USA) and its implications for the Early Triassic recovery. Acta
1066 Palaeontologica Polonica 58, 149-173. http://dx.doi.org/10.4202/app.2011.0060.
1067 Horacek, M., Brandner, R., Abart, R., 2007a. Carbon isotope record of the P/T boundary and
1068 the Lower Triassic in the Southern Alps: Evidence for rapid changes in storage of organic
1069 carbon. Palaeogeography, Palaeoclimatology, Palaeoecology 252, 347-354.
1070 https://doi.org/10.1016/j.palaeo.2006.11.049.
1071 Horacek, M., Richoz, S., Brandner, R., Krystyn, L., Spötl, C., 2007b. Evidence for recurrent
1072 changes in Lower Triassic oceanic circulation of the Tethys: The $\delta^{13}C$ record from marine
1073 sections in Iran. Palaeogeography, Palaeoclimatology, Palaeoecology 252, 355-369.
1074 https://doi.org/10.1016/j.palaeo.2006.11.052.
1075 Jacobs, D.K., Sahagian, D.L., 1993. Climate induced fluctuations in sea level during
1076 nonglacial times. Nature 361, 710-712. https://doi.org/10.1038/361710a0.
1077 Jattiot, R., Brayard, A., Bucher, H., Vennin, E., Caravaca, G., Jenks, J.F., Bylund, K.G.,
1078 Escarguel, G., 2018. Palaeobiogeographical distribution of Smithian (Early Triassic)
1079 ammonoid faunas within the western USA basin and its controlling parameters.
1080 Palaeontology 61, 881-904. https://doi.org/10.1111/pala.12375.
1081 Jattiot, R., Bucher, H., Brayard, A., 2020. Smithian (Early Triassic) ammonoid faunas from
1082 Timor: taxonomy and biochronology. Palaeontographica Abteilung A 317, 1-137. DOI:
1083 10.1127/pala/2020/0096.
1084 Jattiot, R., Bucher, H., Brayard, A., Brosse, M., Jenks, J. F., Bylund, K.G., 2017. Smithian
1085 ammonoid faunas from northeastern Nevada: implications for Early Triassic
1086 biostratigraphy and correlation within the western USA basin. Palaeontographica
1087 Abteilung A 309, 1-89.

1088 Jattiot, R., Bucher, H., Brayard, A., Monnet, C., Jenks, J.F., Hautmann, M., 2016. Revision of
1089 the genus *Anasibirites* Mojsisovics (Ammonoidea): an iconic and cosmopolitan taxon of
1090 the late Smithian (Early Triassic) extinction. Papers in Palaeontology 2, 155-188.
1091 https://doi.org/10.1002/spp2.1036.
1092 Jeffrey, B.M., Elrick, M., Atudorei, V., Lucas, S.G., 2019. Facies architecture and across-
1093 shelf variability of an extensive Lower Triassic (Smithian) microbial carbonate mound
1094 complex in the western U.S. Palaeogeography, Palaeoclimatology, Palaeoecology 521, 42-
1095 56. https://doi.org/10.1016/j.palaeo.2019.02.007.
1096 Jenks, J., Brayard, A., 2018. Smithian (Early Triassic) ammonoids from Crittenden Springs,
1097 Elko County, Nevada: Taxonomy, biostratigraphy and biogeography. New Mexico
1098 Museum of Natural History and Science, Bulletin 78, 1-175.
1099 Jenks, J., Brayard, A., Brühwiler, T., Bucher, H., 2010. New Smithian (Early Triassic)
1100 ammonoids from Crittenden Springs, Elko County, Nevada: Implications for taxonomy,
1101 biostratigraphy and biogeography. New Mexico Museum of Natural History and Science,
1102 Bulletin 48, 1-41.
1103 Jenks, J.F., Monnet, C., Balini, M., Brayard, A., Meier, M., 2015. Biostratigraphy of Triassic
1104 Ammonoids, in: Klug, C. et al. (Eds.), Ammonoid Paleobiology: From macroevolution to
1105 paleogeography, Topics in Geobiology, 44, Springer Netherlands, pp. 329-388.
1106 https://doi.org/10.1007/978-94-017-9633-0_13.
1107 Kershaw, S., 2017. Palaeogeographic variation in the Permian–Triassic boundary
1108 microbialites: a discussion of microbial and ocean processes after the end-Permian mass
1109 extinction. Journal of Palaeogeography 6, 97-107.
1110 https://doi.org/10.1016/j.jop.2016.12.002.
1111 Kummel, B., 1957. Paleoecology of Lower Triassic formations of southeastern Idaho and
1112 adjacent areas. Geological Society of America Memoir 67, 437-468.

1113 Lucas, S.G., Goodspeed, T.H., Estep, J.W., 2007a. Ammonoid biostratigraphy of the Lower
1114 Triassic Sinbad Formation, East-Central Utah. New Mexico Museum of Natural History
1115 and Science Bulletin 40, 103-108.
1116 Lucas, S.G., Krainer, K., Milner, A.R., 2007b. The type section and age of the Timpoweap
1117 Member and stratigraphic nomenclature of the Triassic Moenkopi Group in Southwestern
1118 Utah. New Mexico Museum of Natural History and Science Bulletin 40, 109-117.
1119 Marzolf, J.E., 1993. Palinspastic reconstruction of early Mesozoic sedimentary basins near the
1120 latitude of Las Vegas; implications for the early Mesozoic Cordilleran cratonal margin. In:
1121 Mesozoic Paleogeography of the Western United States, vol. II (eds Dunn, G.C.,
1122 McDougall, K.A.), pp. 433–462. Pacific Section, Society of Economic Paleontologists and
1123 Mineralogists, Field Trip Guidebook 71.
1124 Mata, S.A., Bottjer, D.J., 2011. Origin of Lower Triassic microbialites in mixed carbonate-
1125 siliciclastic successions: Ichnology, applied stratigraphy, and the end-Permian mass
1126 extinction. Palaeogeography, Palaeoclimatology, Palaeoecology 300, 158-178.
1127 https://doi.org/10.1016/j.palaeo.2010.12.022.
1128 Mathews, A.A.L., 1929. The Lower Triassic cephalopod fauna of the Fort Douglas area, Utah.
1129 Walker Museum Memoirs 1, 1-46.
1130 McKee, E.D., 1954. Stratigraphy and history of the Moenkopi Formation of Triassic age.
1131 Geological Society of America, New York.
1132 Monnet, C., De Baets, K., Yaccobucci, M.M., 2015. Buckman's rules of covariation, in: Klug,
1133 C. et al. (Eds.), Ammonoid Paleobiology: From macroevolution to paleogeography, Topics
1134 in Geobiology, 44, Springer Netherlands, pp. 67-94. https://doi.org/10.1007/978-94-017-
1135 9633-0_4.

1136 Nielson, R.L., 1991. Petrology, sedimentology and stratigraphic implications of the Rock
1137 Canyon conglomerate, southwestern Utah. Utah Geological Survey, Miscellaneous
1138 Publication 91, 65pp.
1139 Nielson, R.L., Johnson, J.L., 1979. The Timpoweap Member of the Moenkopi Formation,
1140 Timpoweap Canyon, Utah. Utah Geology 6, 17-27.
1141 Olivier, N., Brayard, A., Fara, E., Bylund, K.G., Jenks, J.F., Vennin, E., Stephen, D.A.,
1142 Escarguel, G., 2014. Smithian shoreline migrations and depositional settings in
1143 Timpoweap Canyon (Early Triassic, Utah, USA). Geological Magazine 151, 938-955.
1144 https://doi.org/10.1017/S0016756813000988.
1145 Olivier, N., Brayard, A., Vennin, E., Escarguel, G., Fara, E., Bylund, K.G., Jenks, J.F.,
1146 Caravaca, G., Stephen, D.A., 2016. Evolution of depositional settings in the Torrey area
1147 during the Smithian (Early Triassic, Utah, USA) and their significance for the biotic
1148 recovery. Geological Journal 51, 600-626. https://doi.org/10.1002/gj.2663.
1149 Olivier, N., Fara, E., Vennin, E., Bylund, K.G., Jenks, J.F., Escarguel, G., Stephen, D.A.,
1150 Goudemand, N., Snyder, D., Thomazo, C., Brayard, A., 2018. Late Smithian microbial
1151 deposits and their lateral marine fossiliferous limestones (Early Triassic, Hurricane Cliffs,
1152 Utah, USA). Facies 64, 13. https://doi.org/10.1007/s10347-018-0526-3.
1153 Orchard, M.J., 2007. Conodont diversity and evolution through the latest Permian and Early
1154 Triassic upheavals. Palaeogeography, Palaeoclimatology, Palaeoecology 252, 93–117.
1155 https://doi.org/10.1016/j.palaeo.2006.11.037.
1156 Paull, R.A., Paull, R.K., 1993. Interpretation of Early Triassic nonmarine-marine relations,
1157 Utah, U.S.A. New Mexico Museum of Natural History and Science Bulletin 3, 403-409.
1158 Paull, R.K., Paull, R.A., 1997. Transgressive conodont faunas of the early Triassic: an
1159 opportunity for correlation in the Tethys and the circum-Pacific, in: Dickins, J.M. et al.
1160 (Eds.), Late Palaeozoic and Early Mesozoic circum-Pacific events and their global

1161 correlation, World and Regional Geology, Vol. 10, Cambridge University Press, New
1162 York, pp. 158-167.
1163 Payne, J.L., Lehrmann, D.J., Wei, J., Orchard, M.J., Schrag, D.P., Knoll, A.H., 2004. Large
1164 perturbations of the carbon cycle during recovery from the end-Permian extinction.
1165 Science 305, 506-509. DOI:10.1126/science.1097023.
1166 Perfili, C.M., Ritter, S.M., 2018. Microbial mounds in the Timpoweap Member of the Lower
1167 Triassic (Smithian) Moenkopi Formation, Hurricane Cliffs, SW Utah. AAPG Annual
1168 Convention and Exhibition.
1169 Piazza, V., 2015. Late Smithian (Early Triassic) ammonoids from the uppermost
1170 Lusitaniadalen Member (Vikinghøgda Formation), Svalbard. Ms. Thesis, University of
1171 Oslo, 135 pp.
1172 Piazza, V., Hammer, Ø., Jattiot, R., 2017. New late Smithian (Early Triassic) ammonoids
1173 from the Lusitandiadalan Member, Vikinghøgda Formation, Svalbard. Norwegian Journal
1174 of Geology 97, 105-117. DOI:10.17850/njg97-2-03.
1175 Poborski, S.J., 1954. Virgin Formation (Triassic) of the St. George, Utah, area. Geological
1176 Society of America Bulletin 65, 971-1006.
1177 Pruss, S.B., Corsetti, F.A., Bottjer, D.J., 2005. The unusual sedimentary rock record of the
1178 Early Triassic: A case study from the southwestern United States. Palaeogeography,
1179 Palaeoclimatology, Palaeoecology 222, 33-52.
1180 https://doi.org/10.1016/j.palaeo.2005.03.007.
1181 Pruss, S.B., Payne, J.L., Bottjer, D.J., 2007. *Planucopsis* bioherms: the first metazoan
1182 buildups following the end-Permian mass extinction. Palaios 22, 17-23.
1183 DOI:10.2110/palo.2005.p05-050r.
1184 Reeside, J.B.Jr., 1943. Letter to the Chief Geologist, U.S. Geological Survey.

1185 Reeside, J.B.Jr., Bassler, H., 1922. Stratigraphic sections in southwestern Utah and
1186 northwestern Arizona. U.S. Geological Survey, Professional Paper 129-D, 53-77.
1187 Romano, C., Goudemand, N., Vennemann, T.W., Ware, D., Schneebeli-Hermann, E.,
1188 Hochuli, P.A., Brühwiler, T., Brinkmann, W., Bucher, H., 2013. Climatic and biotic
1189 upheavals following the end-Permian mass extinction. Nature Geoscience 6, 57-60.
1190 https://doi.org/10.1038/ngeo1667.
1191 Schneebeli-Hermann, E., Bagherpour, B., Vennemann, T., Leu, M., Bucher, H., 2020.
1192 Sedimentary organic matter from a cored Early Triassic succession, Georgetown (Idaho,
1193 USA). Swiss Journal of Palaeontology 139, 5. https://doi.org/10.1186/s13358-020-00205-
1194 9.
1195 Schneebeli-Hermann, E., Hochuli, P.A., Bucher, H., Goudemand, N., Brühwiler, T., Galfetti,
1196 T., 2012. Palynology of the Lower Triassic succession of Tulong, South Tibet — Evidence
1197 for early recovery of gymnosperms. Palaeogeography, Palaeoclimatology, Palaeoecology
1198 339–341, 12-24. https://doi.org/10.1016/j.palaeo.2012.04.010.
1199 Schubert, J.K., Bottjer, D.J., 1995. Aftermath of the Permian-Triassic mass extinction event:
1200 paleoecology of Lower Triassic carbonates in the western USA. Palaeogeography,
1201 Palaeoclimatology, Palaeoecology 116, 1-39. https://doi.org/10.1016/0031-
1202 0182(94)00093-N.
1203 Schulz, M., Schäfer- Neth, C., 1997. Translating Milankovitch climate forcing into eustatic
1204 fluctuations via thermal deep water expansion: a conceptual link. Terra Nova 9, 228-231.
1205 https://doi.org/10.1111/j.1365-3121.1997.tb00018.x.
1206 Shigeta, Y., Komastu, T., Maekawa, T., Dang, H.T., 2014. Olenekian (Early Triassic)
1207 stratigraphy and fossil assemblages in northeastern Vietnam. National Museum of Nature
1208 and Science Monographs, Tokyo.

1209 Shigeta, Y., Zakharov, Y.D., Maeda, H., Popov, A.M., 2009. The Lower Triassic system in
1210 the Abrek Bay area, South Primorye, Russia. National Museum of Nature and Science,
1211 Tokyo.
1212 Song, H., Tong, J., Algeo, T.J., Song, H., Qiu, H., Zhu, Y., Tian, L., Lyons, T.W., Luo, G.,
1213 Kump, L.R., 2014. Early Triassic seawater sulfate drawdown. Geochimica Cosmochimica
1214 Acta 128, 95–113. https://doi.org/10.1016/j.gca.2013.12.009.
1215 Spath, L.F., 1930. The Eotriassic invertebrate fauna of east Greenland. Saertryk af
1216 Meddelelser om Gronland 83, 1-90.
1217 Spath, L.F., 1934. Part 4: The Ammonoidea of the Trias, Catalogue of the fossil Cephalopoda
1218 in the British Museum (Natural History). The Trustees of the British Museum, London.
1219 Stanley, S.M., 2009. Evidence from ammonoids and conodonts for multiple Early Triassic
1220 mass extinctions. Proceedings of the National Academy of Sciences USA 106, 15264-
1221 15267. https://doi.org/10.1073/pnas.0907992106.
1222 Stebbins, A., Algeo, T.J., Olsen, C., Sano, H., Rowe, H., Hannigan, R., 2019. Sulfur-isotope
1223 evidence for recovery of seawater sulfate concentrations from a PTB minimum by the
1224 Smithian-Spathian transition. Earth-Science Reviews 195, 83-95.
1225 https://doi.org/10.1016/j.earscirev.2018.08.010.
1226 Stephen, D.A., Bylund, K.G., Bybee, P.J., Ream, W.J., 2010. Ammonoid beds in the Lower
1227 Triassic Thaynes Formation of western Utah, USA, in: Tanabe, K. et al. (Eds.),
1228 Cephalopods - Present and Past, Tokai University Press, Tokyo, pp. 243-252.
1229 Stewart, J.H., Poole, F.G., Wilson, R.F., 1972. Stratigraphy and origin of the Triassic
1230 Moenkopi Formation and related strata in the Colorado Plateau region. Geological Survey
1231 Professional Paper 691, 195pp.

Sun, Y., Joachimski, M.M., Wignall, P.B., Yan, C., Chen, Y., Jiang, H., Wang, L., Lai, X., 2012. Lethally hot temperatures during the Early Triassic greenhouse. Science 338, 366-370. DOI:10.1126/science.1224126.

Sun, Y.D., Wignall, P.B., Joachimski, M.M., Bond, D.P.G., Grasby, S.E., Sun, S., Yan, C.B., Wang, L.N., Chen, Y.L., Lai, X.L., 2015. High amplitude redox changes in the late Early Triassic of South China and the Smithian–Spathian extinction. Palaeogeography, Palaeoclimatology, Palaeoecology 427, 62-78. https://doi.org/10.1016/j.palaeo.2015.03.038.

Thomazo, C., Brayard, A., Elmeknassi, S., Vennin, E., Olivier, N., Caravaca, G., Escarguel, G., Fara, E., Bylund, K.G., Jenks, J.F., Stephen, D.A., Killingsworth, B., Sansjofre, P., Cartigny, P., 2019. Multiple sulfur isotope signals associated with the late Smithian event and the Smithian/Spathian boundary. Earth-Science Reviews 195, 96-113. https://doi.org/10.1016/j.earscirev.2018.06.019.

Thomazo, C., Vennin, E., Brayard, A., Bour, I., Mathieu, O., Elmeknassi, S., Olivier, N., Escarguel, G., Bylund, K.G., Jenks, J., Stephen, D.A., Fara, E., 2016. A diagenetic control on the Early Triassic Smithian–Spathian carbon isotopic excursions recorded in the marine settings of the Thaynes Group (Utah, USA). Geobiology 14, 220-236. https://doi.org/10.1111/gbi.12174.

Tozer, E.T., 1971. Triassic time and ammonoids: Problems and proposals. Canadian Journal of Earth Sciences 8, 989-1031. https://doi.org/10.1139/e71-088.

Tozer, E.T., 1981. Triassic Ammonoidea: classification, evolution and relationship with Permian and Jurassic forms, in: House, M.R., Senior, J.R. (Eds.), The Ammonoidea, The Systematics Association, London, pp. 65-100.

1255 Tozer, E.T., 1982. Marine Triassic faunas of North America: their significance for assessing
1256 plate and terrane movements. Geologische Rundschau 71, 1077-1104.
1257 https://doi.org/10.1007/BF01821119.
1258 Tozer, E.T., 1994. Canadian Triassic ammonoid faunas. Geologic Survey of Canada Bulletin
1259 467, 1-663.
1260 Vennin, E., Olivier, N., Brayard, A., Bour, I., Thomazo, C., Escarguel, G., Fara, E., Bylund,
1261 K.G., Jenks, J.F., Stephen, D.A., Hofmann, R., 2015. Microbial deposits in the aftermath of
1262 the end-Permian mass extinction: A diverging case from the Mineral Mountains (Utah,
1263 USA). Sedimentology 62, 753-792. https://doi.org/10.1111/sed.12166.
1264 Wang, Y.G., He, G.X., 1976. Triassic ammonoids from Mount Jolmo Lung region. Scientific
1265 Report of Excursion in Mount Jolmo Lungma Region, Paleontology 3, 223-438.
1266 Ware, D., Bucher, H., Brayard, A., Schneebeli-Hermann, E., Brühwiler, T., 2015. High-
1267 resolution biochronology and diversity dynamics of the Early Triassic ammonoid recovery:
1268 The Dienerian faunas of the Northern Indian Margin. Palaeogeography, Palaeoclimatology,
1269 Palaeoecology 440, 363-373. https://doi.org/10.1016/j.palaeo.2015.09.013.
1270 Westermann, G.E.G., 1966. Covariation and taxonomy of the Jurassic ammonite *Sonninia*
1271 *adicra* (Waagen). Neues Jahrbuch für Geologie und Paläontologie, Abhandlungen 124,
1272 289-312.
1273 Zakharov, Y.D., 1978. Lower Triassic ammonoids of East USSR. Nauka, Moscow, 220 pp.
1274 Zakharov, Y.D., Abnavi, N.M., 2013. The ammonoid recovery after the end-Permian mass
1275 extinction: Evidence from the Iran-Transcaucasia area, Siberia, Primorye, and Kazakhstan.
1276 Acta Palaeontologica Polonica 58, 127-147. http://dx.doi.org/10.4202/app.2011.0054.
1277 Zhang, L., Orchard, M.J., Brayard, A., Algeo, T.J., Zhao, L., Chen, Z.-Q., Lyu, Z., 2019. The
1278 Smithian/Spathian boundary (late Early Triassic): A review of ammonoid, conodont, and

carbon-isotopic criteria. Earth-Science Reviews 195, 7-36. https://doi.org/10.1016/j.earscirev.2019.02.014.

Zhang, L., Zhao, L., Chen, Z.Q., Algeo, T.J., Li, Y., Cao, L., 2015. Amelioration of marine environments at the Smithian–Spathian boundary, Early Triassic. Biogeosciences 12, 1597-1613. https://doi.org/10.5194/bg-12-1597-2015.

Zhao, H., Algeo, T.J., Liu, Y., Chen, Z.-Q., Zhang, L., Hu, Z., Li, Z., 2020. Lower Triassic carbonate $\delta^{238}U$ record demonstrates expanded oceanic anoxia during Smithian Thermal Maximum and improved ventilation during Smithian-Spathian boundary cooling event. Palaeogeography, Palaeoclimatology, Palaeoecology 539, 109393. https://doi.org/10.1016/j.palaeo.2019.109393.

Figure captions

Fig. 1. Early Triassic (A) and present-day (B) locations of the western USA basin. C) Schematic distribution of depositional environments within the southern part of the western USA basin during the Smithian. D-F) Map of southern Utah and northern Arizona showing the location of the sampled localities.

Fig. 2. Stratigraphic logs showing the main faunal occurrences at Workman Wash and Honeymoon Trail (Washington County, Utah). Stratigraphy follows the main units defined by Lucas et al. (2007b) and described by Brayard et al. (2015), Olivier et al. (2018) and Jeffrey et al. (2019). RCC: Rock Canyon Conglomerate.

Fig. 3. Stratigraphic logs showing the main faunal occurrences at Rock Canyon (Arizona) and White Sage Wash (Utah). See Fig. 2 for references and legends.

Fig. 4. Temporal extent of the deposition of the Sinbad Fm. at each studied locality as determined by newly-found ammonoid assemblages. See Fig. 1 for abbreviations. The gray shaded area corresponds to the end of the marine deposits of the Sinbad Fm. The age for the base of the Sinbad Fm. at WW remains tentative because late middle Smithian ammonoids have not yet been found at this locality.

Fig. 5. A–M: *Guodunites hooveri*. N–P: *Guodunites monneti*. Specimens A–C and N–O from bed WSW3, White Sage Wash, Utah, late middle Smithian. Specimens D–M and P from bed ROC2-A, late middle Smithian. A: UBGD 32220; B: UBGD 32221; C: suture line of UBGD 32221 at H = 12.7 mm; D–F: UBGD 32222–32224; G–H: lateral and ventral views of UBGD 32225; I: UBGD 32226; J–K: lateral and ventral views of UBGD 32227; L–M: lateral and ventral views of UBGD 32228; N: UBGD 32229; O: suture line of UBGD 32229 at H = 9.3 mm; P: UBGD 32230. Black arrows indicate the position of the corresponding ventral view. Scale bars: 10 mm, except C and O: 5 mm.

Fig. 6. A–Q: *Gurleyites smithi*. All specimens from bed BRC, Workman Wash, Utah, early late Smithian. A–D: lateral, apertural and ventral views of UBGD 32232; E–F: lateral and ventral views of UBGD 32233; G–H: lateral and ventral views of UBGD 32234; I: UBGD 32235; J: UBGD 32236; K: UBGD 32237; L–M: lateral and ventral views of UBGD 32238; N: lateral view of two specimens on block UBGD 32239; O: ventral view of the specimen on the left of UBGD 32239; P–Q: lateral and ventral views of UBGD 32240. Black arrows

indicate the position of the corresponding ventral view. Note presence of ventral strigation in A, D, H and O. Scale bars: 10 mm.

Fig. 7. A–S: *Gurleyites smithi*. All specimens from bed BRC, Workman Wash, Utah, early late Smithian. A–B: lateral and ventral views of UBGD 32241; C–D: lateral and ventral views of UBGD 32242; E–F: lateral and ventral views of UBGD 32243; G: UBGD 32244; H–I: lateral and ventral views of UBGD 32245; J: UBGD 32246; K: UBGD 32247; L–M: lateral and ventral views of UBGD 32248; N–P: lateral, ventral and apertural views of UBGD 32249; Q–S: lateral and ventral views of UBGD 32250. Black arrow indicates the position of the corresponding ventral view. Scale bars: 10 mm.

Fig. 8. A–O: *Gurleyites smithi*. All specimens from bed BRC, Workman Wash, Utah, early late Smithian. A: UBGD 32251; B–C: lateral and ventral views of UBGD 32252; D–E: lateral and ventral views of UBGD 32253; F–G: lateral and ventral views of UBGD 32254; H: UBGD 32255; I: UBGD 32256 (specimen in the background is probably *Hemiprionites typus*); J: UBGD 32257; K: UBGD 32258; L–M: lateral and ventral views of UBGD 32259; N–O: lateral and ventral views of UBGD 32260. Black arrows indicate the position of the corresponding ventral view. Identification of UBGD 32259 (L–M) and UBGD 32260 (N–O) may be questionable as outer whorls overlap with intraspecific variation of *Hemiprionites typus*, but their overall shape and ornamentation, especially folds on inner whorls, fit within *G. smithi*. Scale bars: 10 mm.

Fig. 9. A–J: *Gurleyites smithi*. All specimens from bed BRC, Workman Wash, Utah, early late Smithian. A–B: lateral and ventral views of UBGD 32261; C–E: apertural, ventral and lateral views of UBGD 32262; F–G: lateral and ventral views of UBGD 32263; H: suture line

of UBGD 32264 at H = 16.3 mm; I–J: lateral and ventral views of UBGD 32265. K–L: *Wasatchites perrini*. Lateral (K) and ventral (L) views of specimen UBGD 32231, from bed BRC, Workman Wash, Utah, early late Smithian. Black arrow indicates the position of the corresponding ventral view. Scale bar: 10 mm.

Fig. 10. A–H: blocks with *Gurleyites smithi* and *Hemiprionites typus*. All specimens from bed BRC, Workman Wash, Utah, early late Smithian. A–B: lateral and ventral views of specimens on block UBGD 32266; C: lateral view of specimens on block UBGD 32267; D: lateral view of specimens on block UBGD 32268; E–G: lateral and ventral views of specimens on block UBGD 32269; H: suture line of the complete specimen on UBGD 32269 at H = 18.8 mm. Black arrows indicate the position of the corresponding ventral view. Gu: *Gurleyites smithi*; He: *Hemiprionites typus*. Identification of the complete specimen on block UBGD 32269 (E–G) may be questionable as its overall shape, especially coiling, and ornamentation on inner whorls (bullate ribs visible on the umbilical margin) fit within the intraspecific variation of *G. smithi*, but the lack of ornamentation at later growth stages fits with *H. typus*. Its suture line (H) is also somewhat intermediate between *G. smithi* and *H. typus*. Scale bars: 10 mm, except H: 5 mm.

Fig. 11. A–P: *Anasibirites multiformis*. All specimens from bed BRC, Workman Wash, Utah, early late Smithian. A: UBGD 32270; B–C: lateral and ventral views of UBGD 32271; D: UBGD 32272; E: UBGD 32273; F–H: lateral and ventral views of UBGD 32274; I: UBGD 32275; J–L: lateral and ventral views of UBGD 32276; M: UBGD 32277; N: UBGD 32278; O–P: lateral and ventral views of UBGD 32279. Black arrows indicate the position of the corresponding ventral view. Scale bars: 10 mm.

Fig. 12. A–I: *Hemiprionites walcotti*. A–B: lateral and ventral views of UBGD 32280; C–D: lateral and ventral views of UBGD 32281; E: UBGD 32282; F–G: lateral and ventral views of UBGD 32283; H–I: lateral and ventral views of UBGD 32284. J–S: *Hemiprionites typus.* J–K: lateral and ventral views of UBGD 32285; L–M: lateral and ventral views of UBGD 32286; N: lateral view of UBGD 32287 (star indicates the minute depression visible near the ventrolateral margin); O: suture line of UBGD 32288 at H = 15.4 mm; P: lateral view of UBGD 32289; Q: lateral view of UBGD 32290; R–S: lateral and ventral views of UBGD 32291. All specimens from bed BRC, Workman Wash, Utah, early late Smithian. Black arrows indicate the position of the corresponding ventral view. Scale bars: 10 mm, except O: 5 mm.

Supplementary Figure A. Scatter diagrams of H, W and U, and H/D, W/D and U/D for *Guodunites hooveri*. Open symbols indicate specimens from Rock Canyon, Arizona, and White Sage Wash, Utah (n = 12). Grey symbols indicate specimens from central and western Utah (data from Brayard et al., 2013; n = 56) and Palomino Ridge (data from Jattiot et al., 2017; n = 4).

Supplementary Figure B. Scatter diagrams of H, W and U, and H/D, W/D and U/D for *Gurleyites smithi*. Open symbols indicate specimens from bed BRC, Workman Wash, Utah, early late Smithian (n = 40). Grey symbols indicate specimens from Palomino Ridge (data from Jattiot et al., 2017; n = 7) and Crittenden Springs (Jenks and Brayard, 2018; n = 14), Nevada.

Supplementary Figure C. Box plots of U/D for *Gurleyites smithi* and *Hemiprionites typus* from the studied area and Nevada. Specimens from Nevada were sampled at Palomino Ridge (Jattiot et al., 2017) and Crittenden Springs (Jenks and Brayard, 2018).

Supplementary Figure D. Scatter diagrams of H, W and U, and H/D, W/D and U/D for *Anasibirites multiformis*. Open symbols indicate specimens from bed BRC, Workman Wash, Utah, early late Smithian (n = 14). Grey symbols indicate specimens from Palomino Ridge, Nevada (data from Jattiot et al., 2017; n = 54).

Supplementary Figure E. Scatter diagrams of H, W and U, and H/D, W/D and U/D for *Hemiprionites typus*. Open symbols indicate specimens from bed BRC, Workman Wash, Utah, early late Smithian (n = 6). Grey symbols indicate specimens from Palomino Ridge (data from Jattiot et al., 2017; n = 58) and Crittenden Springs (data from Jenks and Brayard, 2018; n = 23), Nevada.

Supplementary Figure F. Scatter diagrams of H, W and U, and H/D, W/D and U/D for *Hemiprionites walcotti*. Open symbols indicate specimens from bed BRC, Workman Wash, Utah, early late Smithian (n = 5). Grey symbols indicate specimens from Palomino Ridge (data from Jattiot et al., 2017; n = 26) and Crittenden Springs (data from Jenks and Brayard, 2018; n = 2), Nevada.

Supplementary Table A. Measurements of some Smithian ammonoids from the studied area, central and southern Utah (data from Brayard et al., 2013) and Nevada (Palomino Ridge and Crittenden Springs; data from Jattiot et al., 2017 and Jenks and Brayard, 2018, respectively) (D: Diameter; H: whorl height; W: whorl width; U: umbilical diameter).

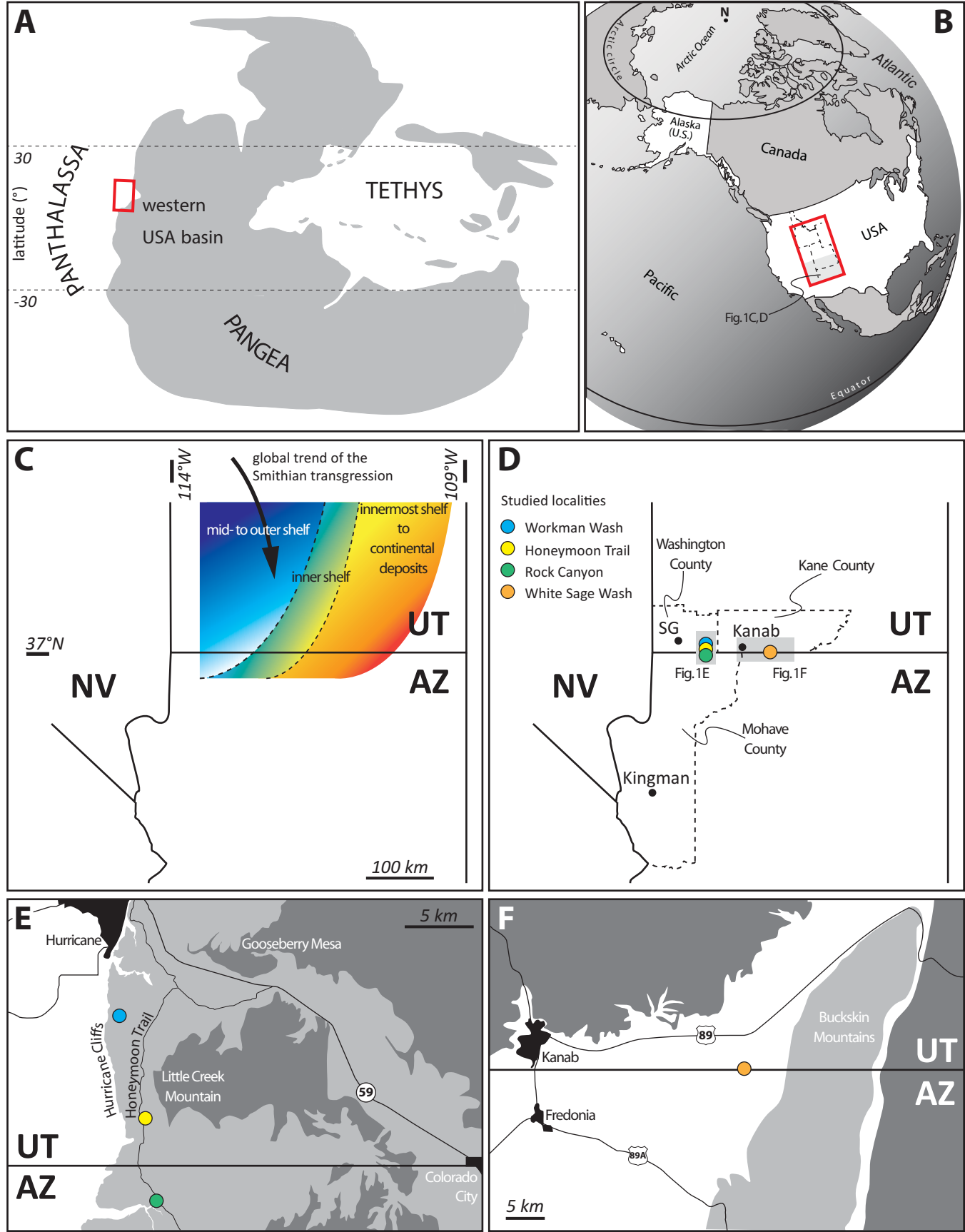
A
30
latitude (°)
-30
PANTHALASSA
western
USA basin
TETHYS
PANGEA
B
N
Arctic circle
Arctic Ocean
Atlantic
Alaska (U.S.)
Canada
USA
Pacific
Fig.1C,D
Equator
C
114°W
109°W
global trend of the Smithian transgression
mid- to outer shelf
inner shelf
innermost shelf to continental deposits
37°N
NV
UT
AZ
100 km
D
Studied localities
Workman Wash
Honeymoon Trail
Rock Canyon
White Sage Wash
Washington County
Kane County
SG
Kanab
Fig.1E
Fig.1F
NV
UT
AZ
Mohave County
Kingman
E
5 km
Hurricane
Gooseberry Mesa
Hurricane Cliffs
Honeymoon Trail
Little Creek Mountain
59
UT
AZ
Colorado City
F
89
Kanab
Buckskin Mountains
UT
AZ
Fredonia
89A
5 km

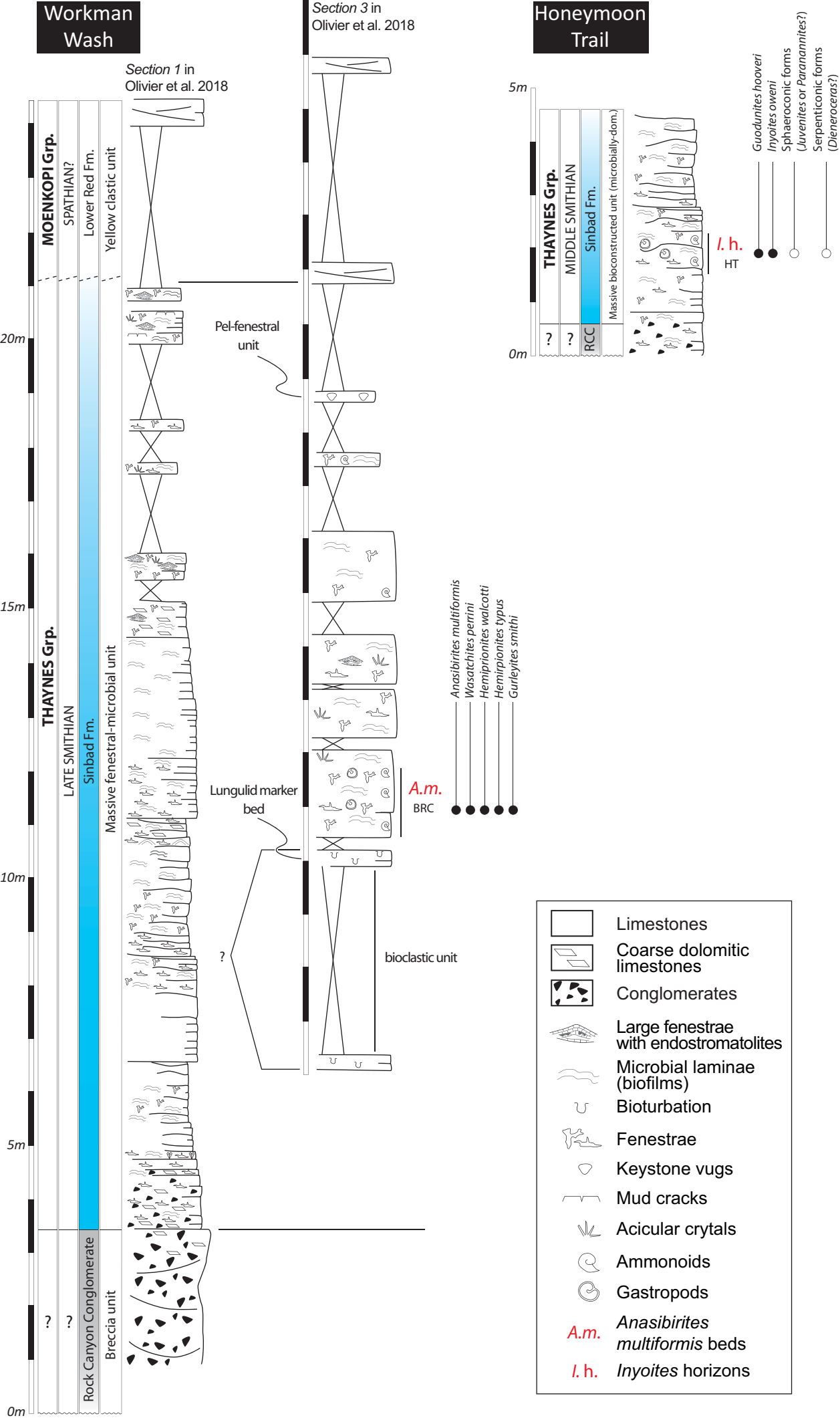
Workman Wash
Section 1 in Olivier et al. 2018
Section 3 in Olivier et al. 2018
Honeymoon Trail
MOENKOPI Grp.
SPATHIAN?
Lower Red Fm.
Yellow clastic unit
THAYNES Grp.
LATE SMITHIAN
Sinbad Fm.
Massive fenestral-microbial unit
Rock Canyon Conglomerate
Breccia unit
Pel-fenestral unit
Lungulid marker bed
bioclastic unit
A.m.
BRC
Anasibirites multiformis
Wasatchites perrini
Hemiprionites walcotti
Hemirpionites typus
Gurleyites smithi
20m
15m
10m
5m
0m
THAYNES Grp.
MIDDLE SMITHIAN
Sinbad Fm.
RCC
Massive bioconstructed unit (microbially-dom.)
I. h.
HT
Guodunites hooveri
Inyoites oweni
Sphaeroconic forms (Juvenites or Paranannites?)
Serpenticonic forms (Dieneroceras?)
Limestones
Coarse dolomitic limestones
Conglomerates
Large fenestrae with endostromatolites
Microbial laminae (biofilms)
Bioturbation
Fenestrae
Keystone vugs
Mud cracks
Acicular crytals
Ammonoids
Gastropods
A.m. Anasibirites multiformis beds
I. h. Inyoites horizons

White Sage Wash

0m 5m

THAYNES Grp.

MIDDLE SMITHIAN

Sinbad Fm.

Massive bioconstructed unit (microbially-dominated)

WSW1 WSW2 WSW3 *l.* h.

Guodunites hooveri

Guodunites monneti

Serpenticonic form (*Dieneroceeras?*)

Rock Canyon

0m 5m 10m

? **THAYNES Grp.**

? MIDDLE SMITHIAN LATE SMITHIAN

Rock Canyon Conglomerate Sinbad Fm.

Conglomeratic unit Massive bioconstructed unit (microbially-dominated)

ROC2-A *l.* h. ROC3-A *A.m.*

Guodunites hooveri

Guodunites monneti

Anasibirites multiformis

Wasatchites perrini

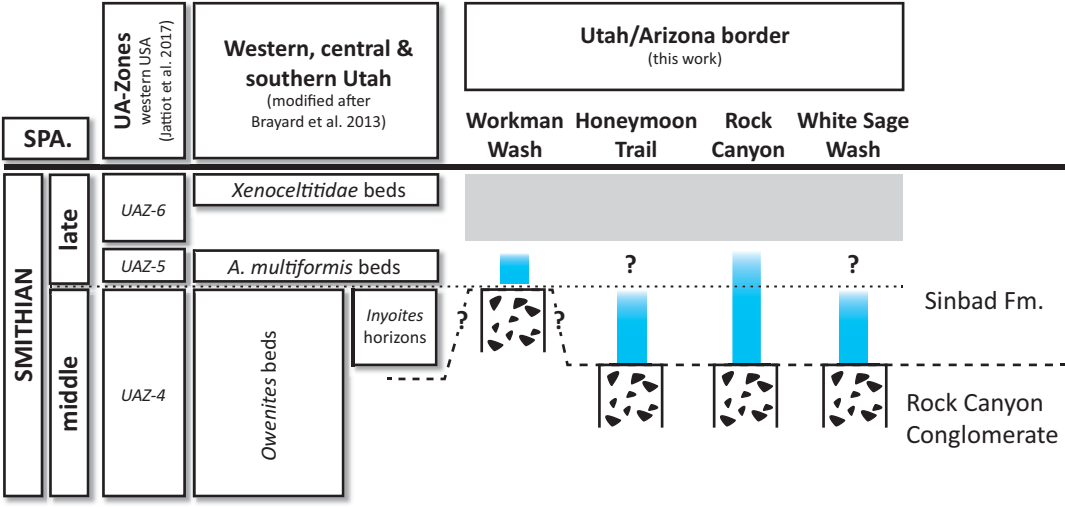
SPA.
UA-Zones
western USA
(Jattiot et al. 2017)
Western, central & southern Utah
(modified after Brayard et al. 2013)
Utah/Arizona border
(this work)
Workman Wash
Honeymoon Trail
Rock Canyon
White Sage Wash
SMITHIAN
late
middle
UAZ-6
UAZ-5
UAZ-4
Xenoceltitidae beds
A. multiformis beds
Owenites beds
Inyoites horizons
?
Sinbad Fm.
Rock Canyon Conglomerate

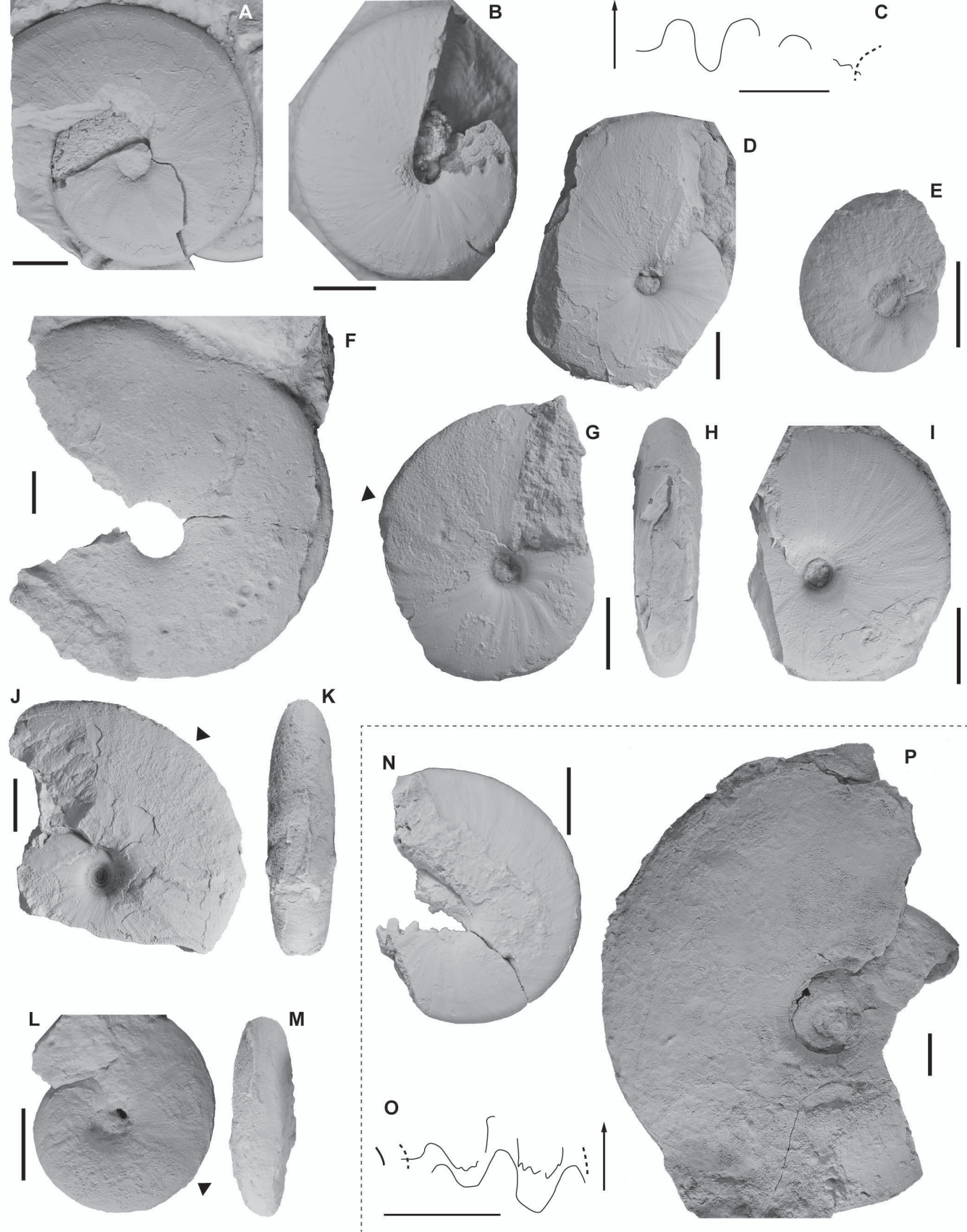
A
B
C
D
E
F
G
H
I
J
K
L
M
N
O
P

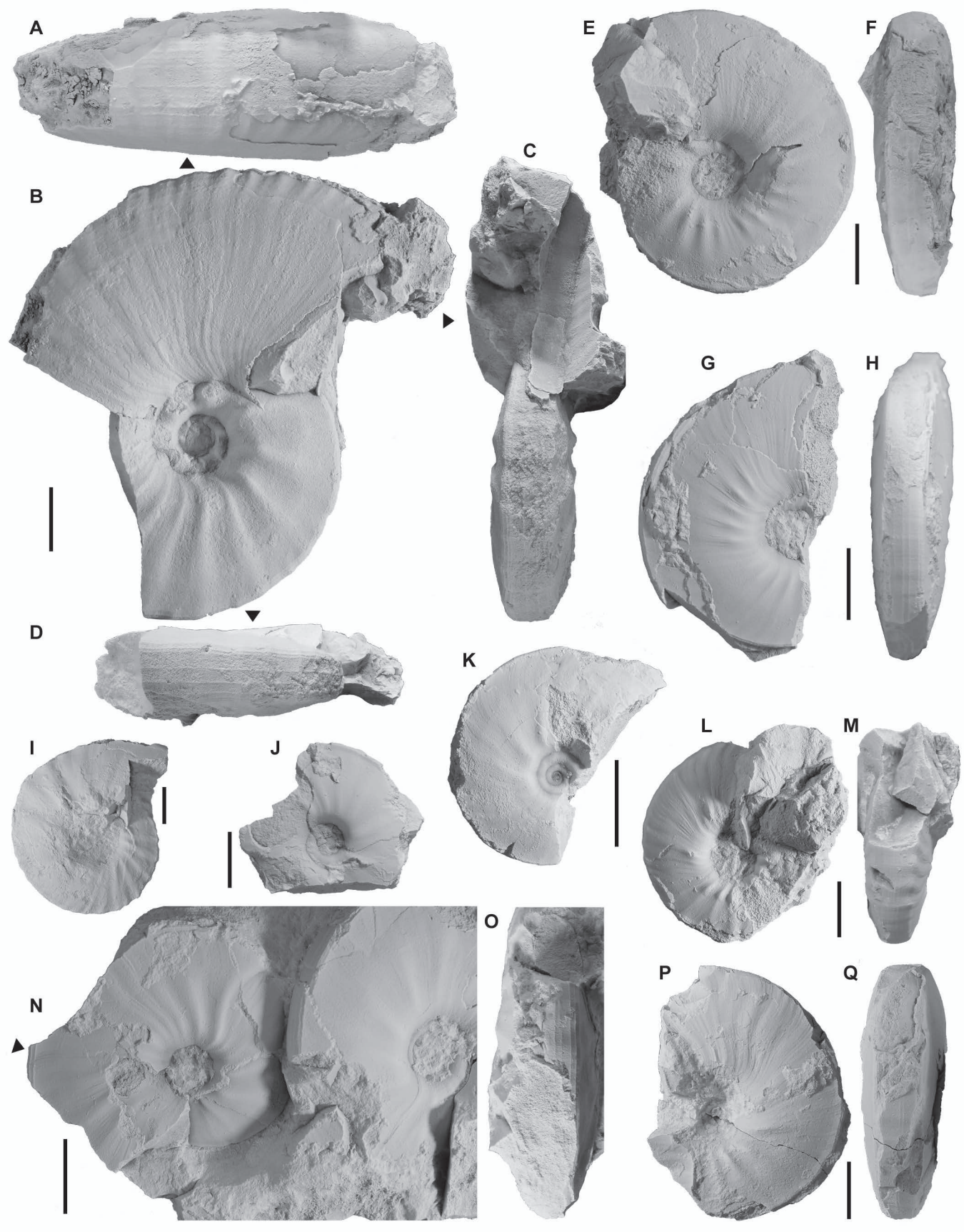
A
B
C
D
E
F
G
H
I
J
K
L
M
N
O
P
Q

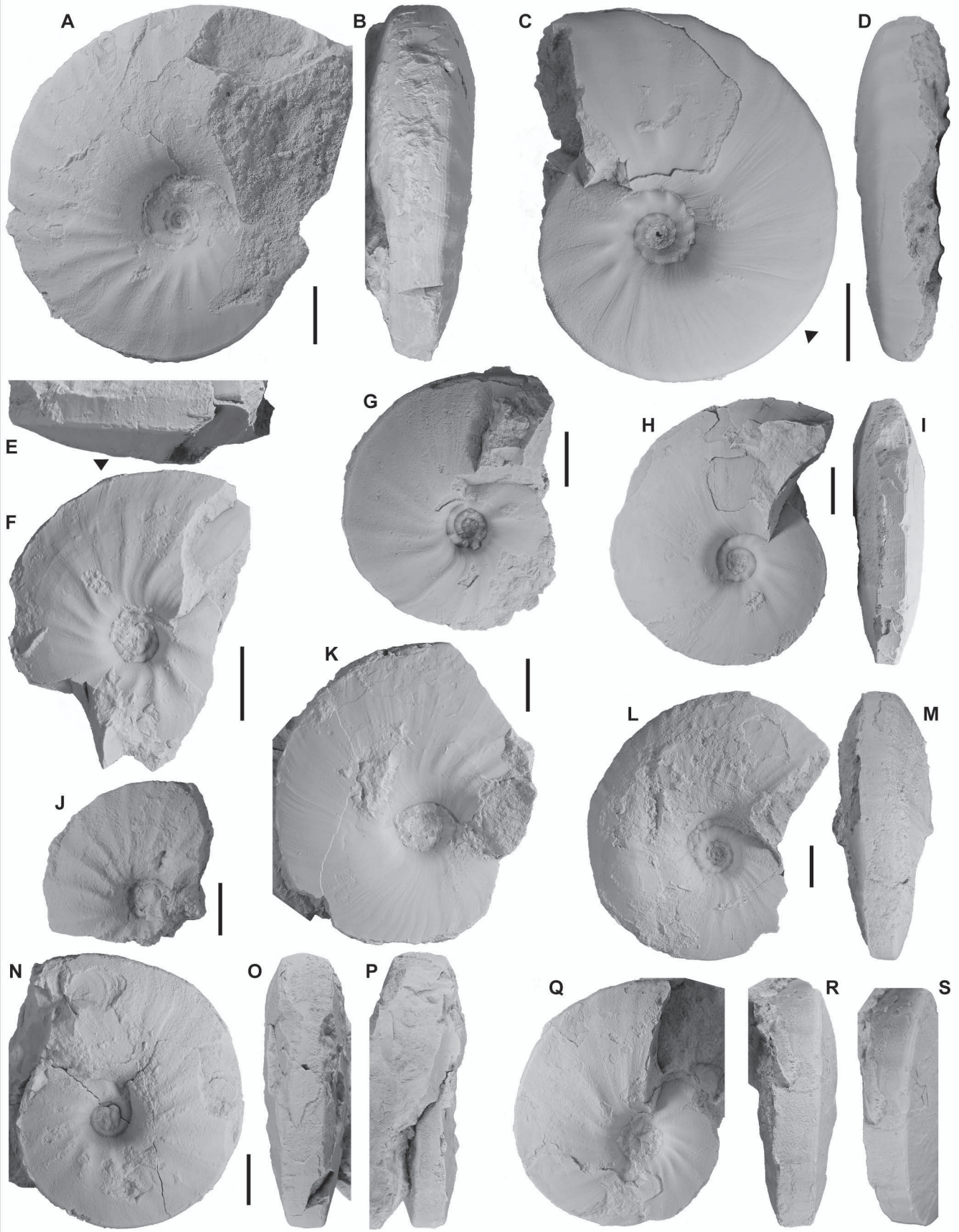
A
B
C
D
E
F
G
H
I
J
K
L
M
N
O
P
Q
R
S

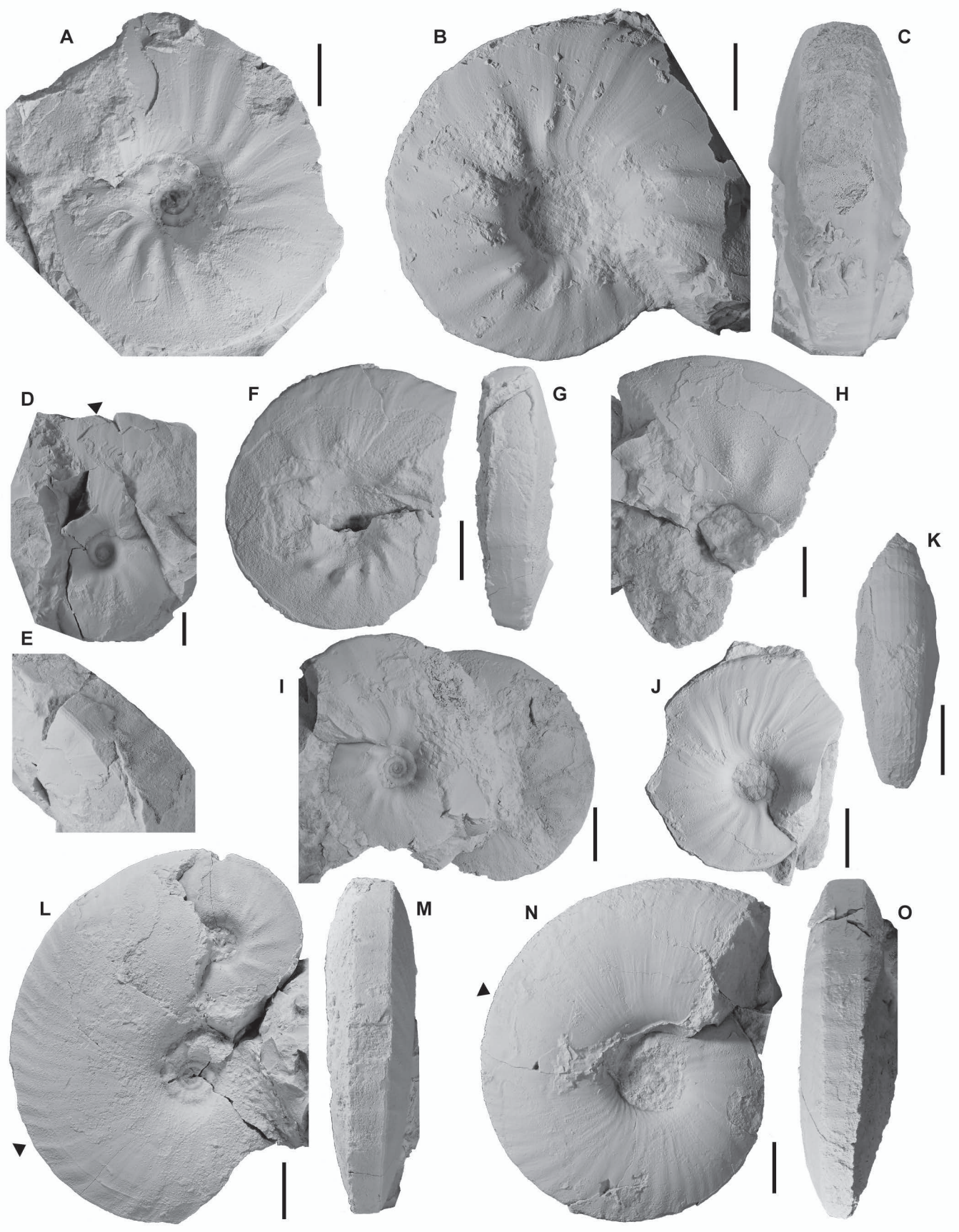
A
B
C
D
F
G
H
K
E
I
J
L
M
N
O

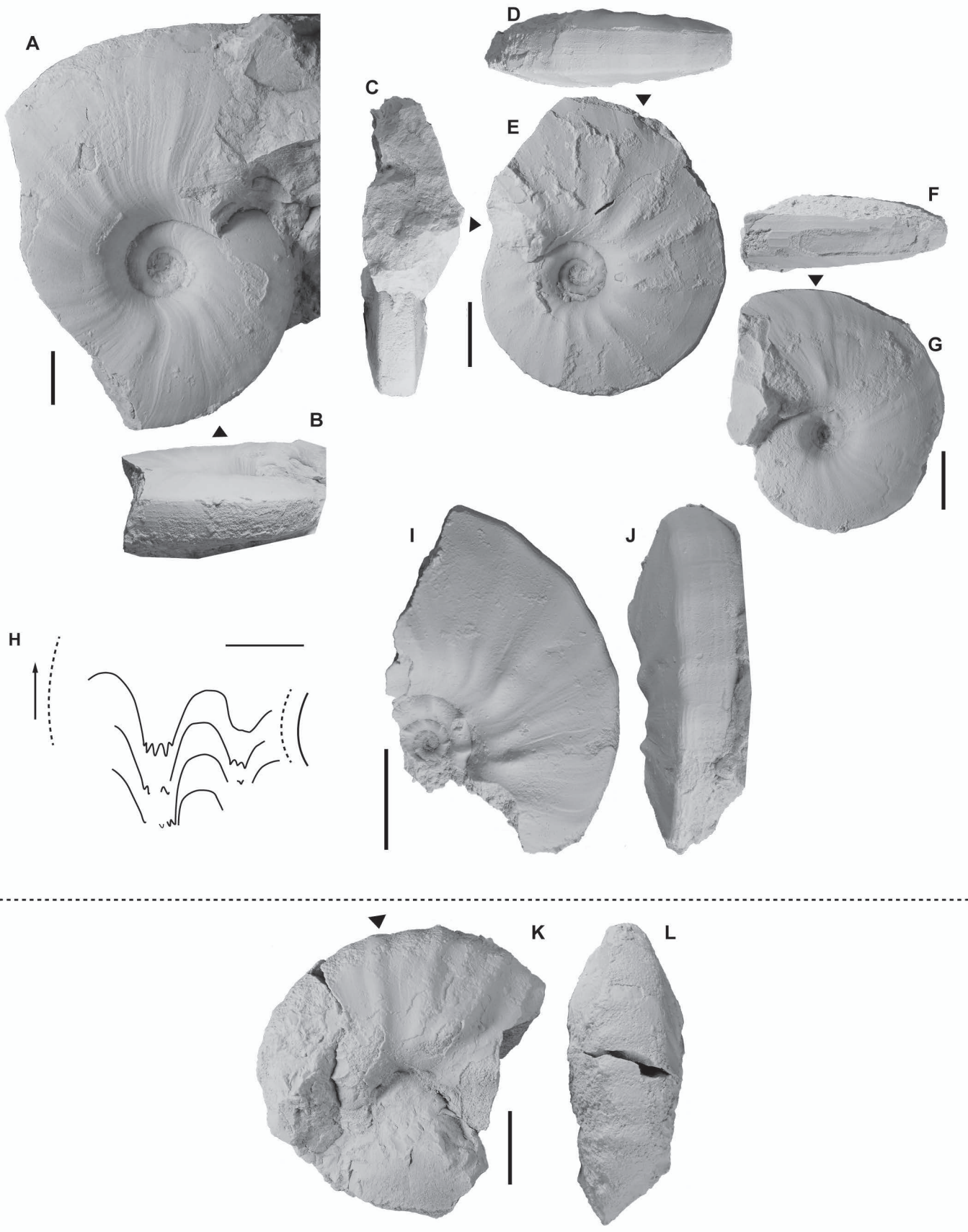
A
B
C
D
E
F
G
H
I
J
K
L

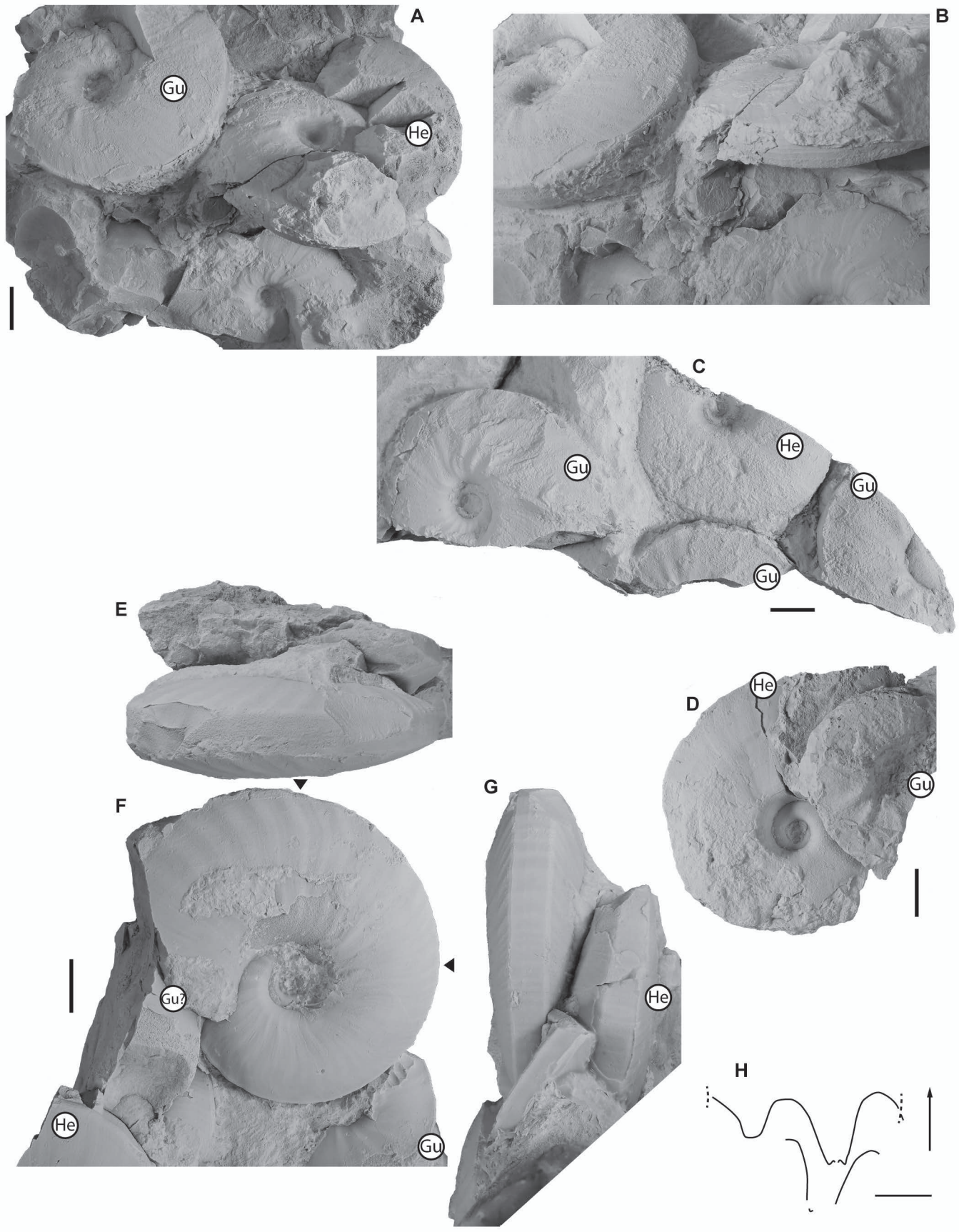
A
Gu
He
B
C
Gu
He
Gu
Gu
E
D
He
Gu
F
G
Gu?
He
He
Gu
H

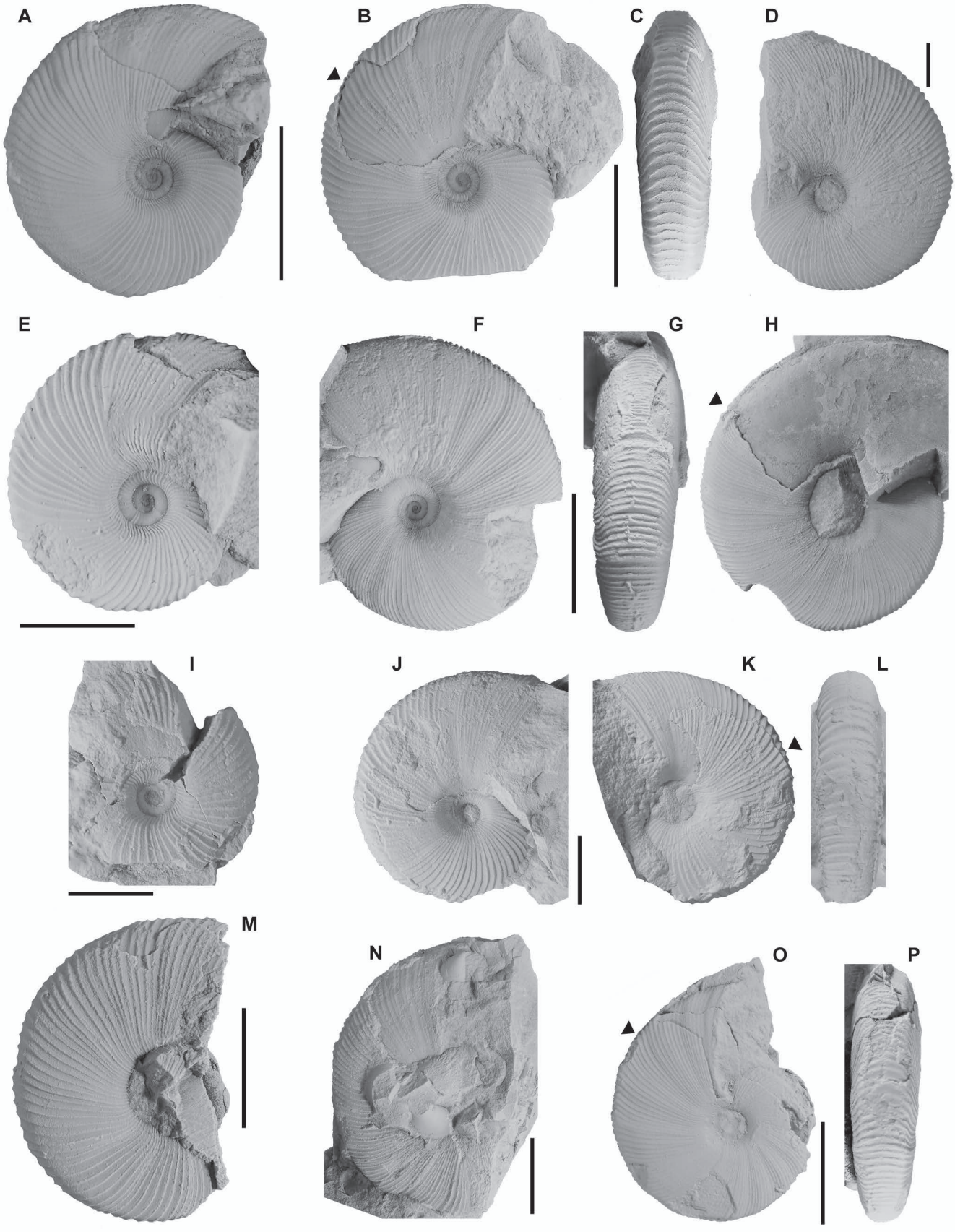
A
B
C
D
E
F
G
H
I
J
K
L
M
N
O
P

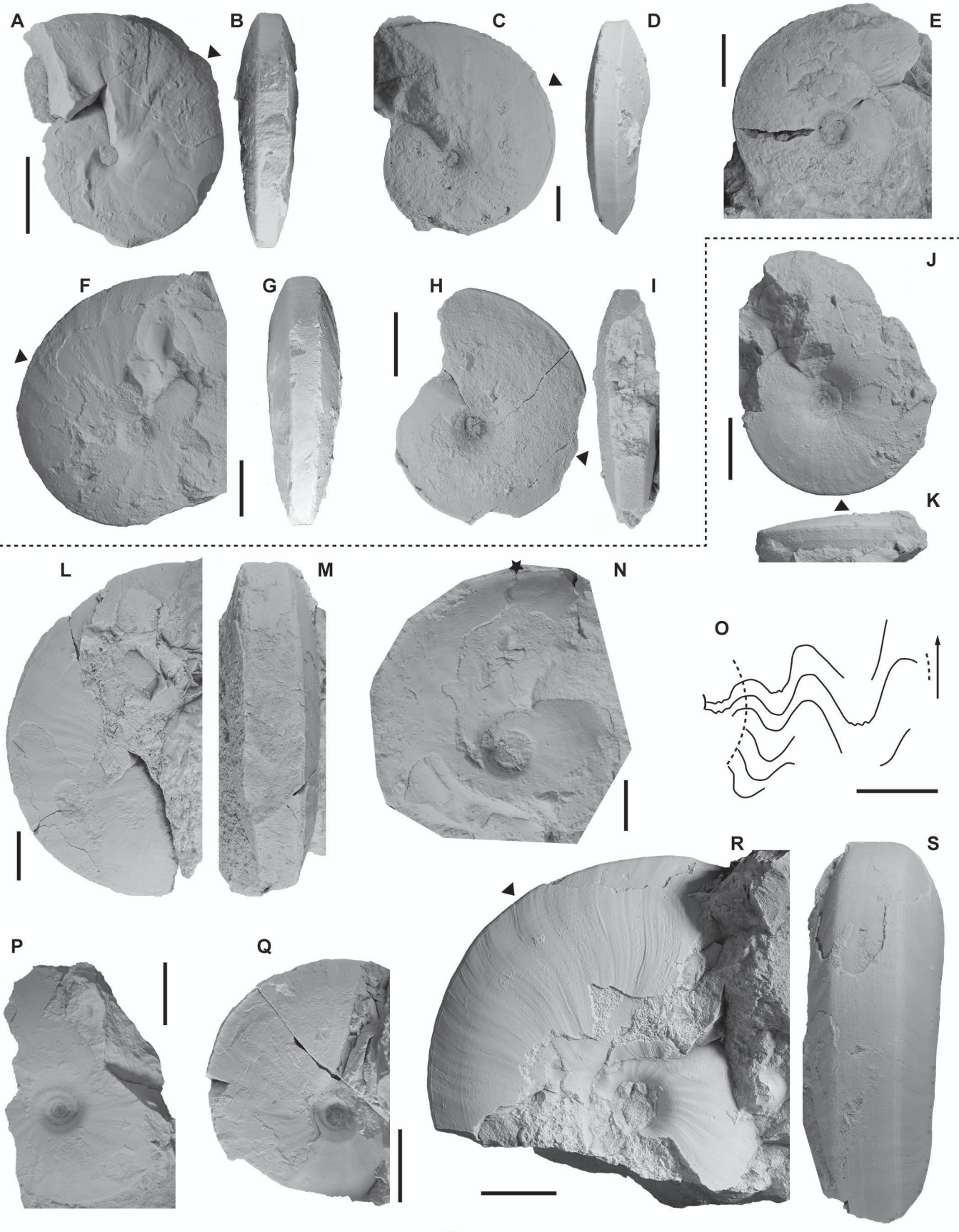
A
B
C
D
E
F
G
H
I
J
K
L
M
N
O
P
Q
R
S

New middle and late Smithian ammonoid faunas from the Utah/Arizona border: new evidence for calibrating Early Triassic transgressive-regressive trends and paleobiogeographical signals in the western USA basin – Brayard et al.

Suppl. Fig. A. Scatter diagrams of H, W and U, and H/D, W/D and U/D for *Guodunites hooveri*. Open symbols indicate specimens from Rock Canyon, Arizona, and White Sage Wash, Utah (n = 12). Grey symbols indicate specimens from central and western Utah (data from Brayard et al., 2013; n = 56) and Palomino Ridge (data from Jattiot et al., 2017; n = 4).

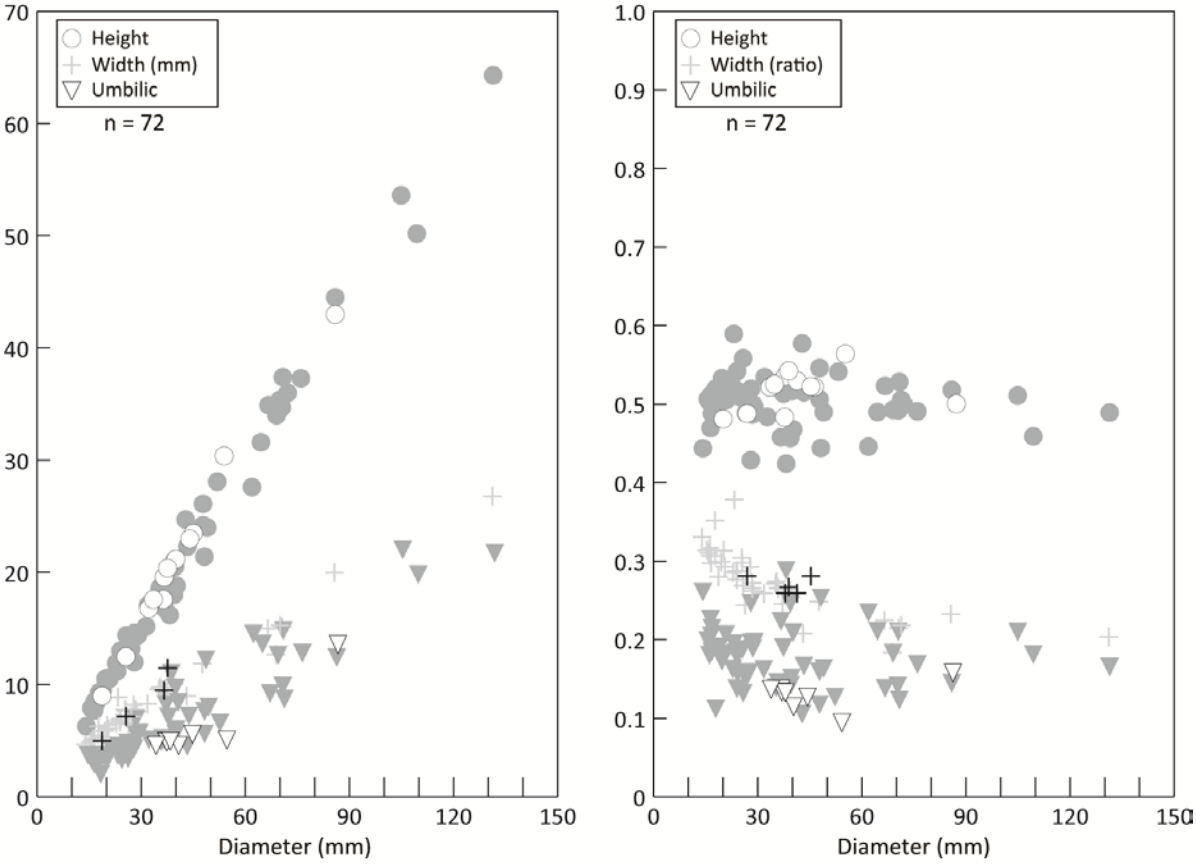

New middle and late Smithian ammonoid faunas from the Utah/Arizona border: new evidence for calibrating Early Triassic transgressive-regressive trends and paleobiogeographical signals in the western USA basin – Brayard et al.

Suppl. Fig. B. Scatter diagrams of H, W and U, and H/D, W/D and U/D for *Gurleyites smithi*. Open symbols indicate specimens from bed BRC, Workman Wash, Utah, early late Smithian (n = 40). Grey symbols indicate specimens from Palomino Ridge (data from Jattiot et al., 2017; n = 7) and Crittenden Springs (Jenks and Brayard, 2018; n = 14), Nevada.

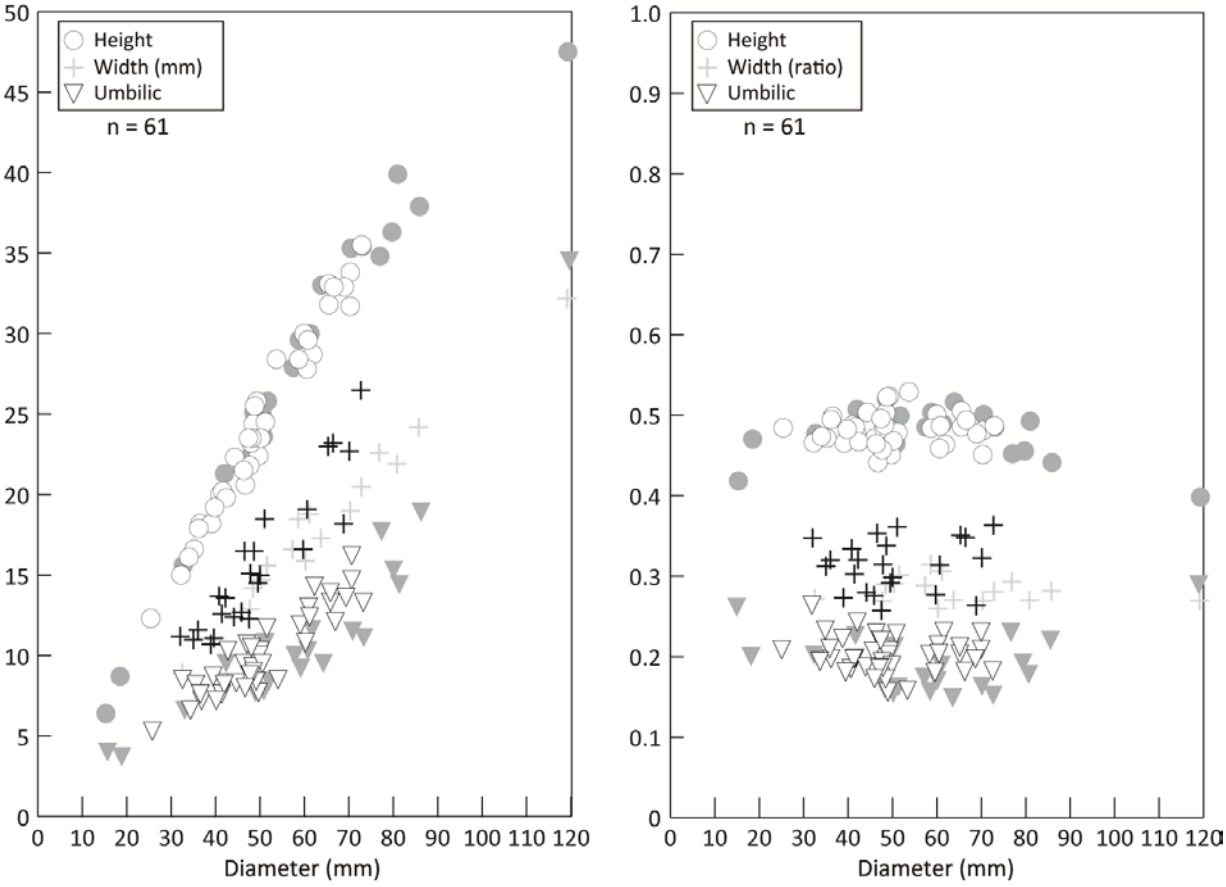

New middle and late Smithian ammonoid faunas from the Utah/Arizona border: new evidence for calibrating Early Triassic transgressive-regressive trends and paleobiogeographical signals in the western USA basin – Brayard et al.

Suppl. Fig. C. Box plots of U/D for *Gurleyites smithi* and *Hemiprionites typus* from the studied area and Nevada. Specimens from Nevada were sampled at Palomino Ridge (Jattiot et al., 2017) and Crittenden Springs (Jenks and Brayard, 2018).

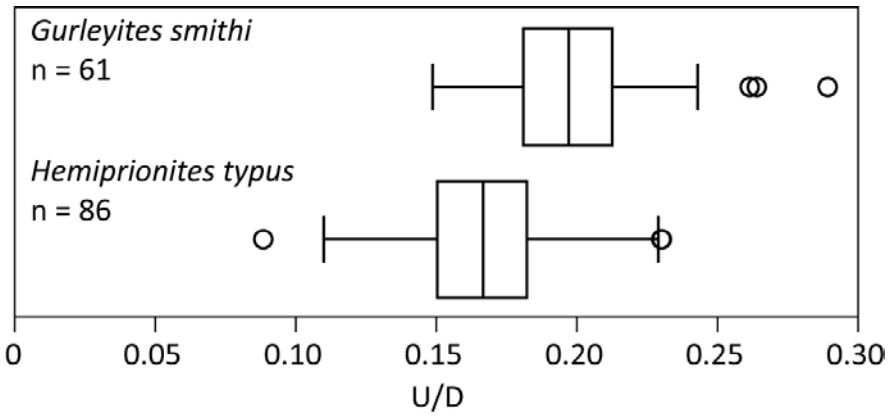

New middle and late Smithian ammonoid faunas from the Utah/Arizona border: new evidence for calibrating Early Triassic transgressive-regressive trends and paleobiogeographical signals in the western USA basin – Brayard et al.

Suppl. Fig. D. Scatter diagrams of H, W and U, and H/D, W/D and U/D for *Anasibirites multiformis*. Open symbols indicate specimens from bed BRC, Workman Wash, Utah, early late Smithian (n = 14). Grey symbols indicate specimens from Palomino Ridge, Nevada (data from Jattiot et al., 2017; n = 54).

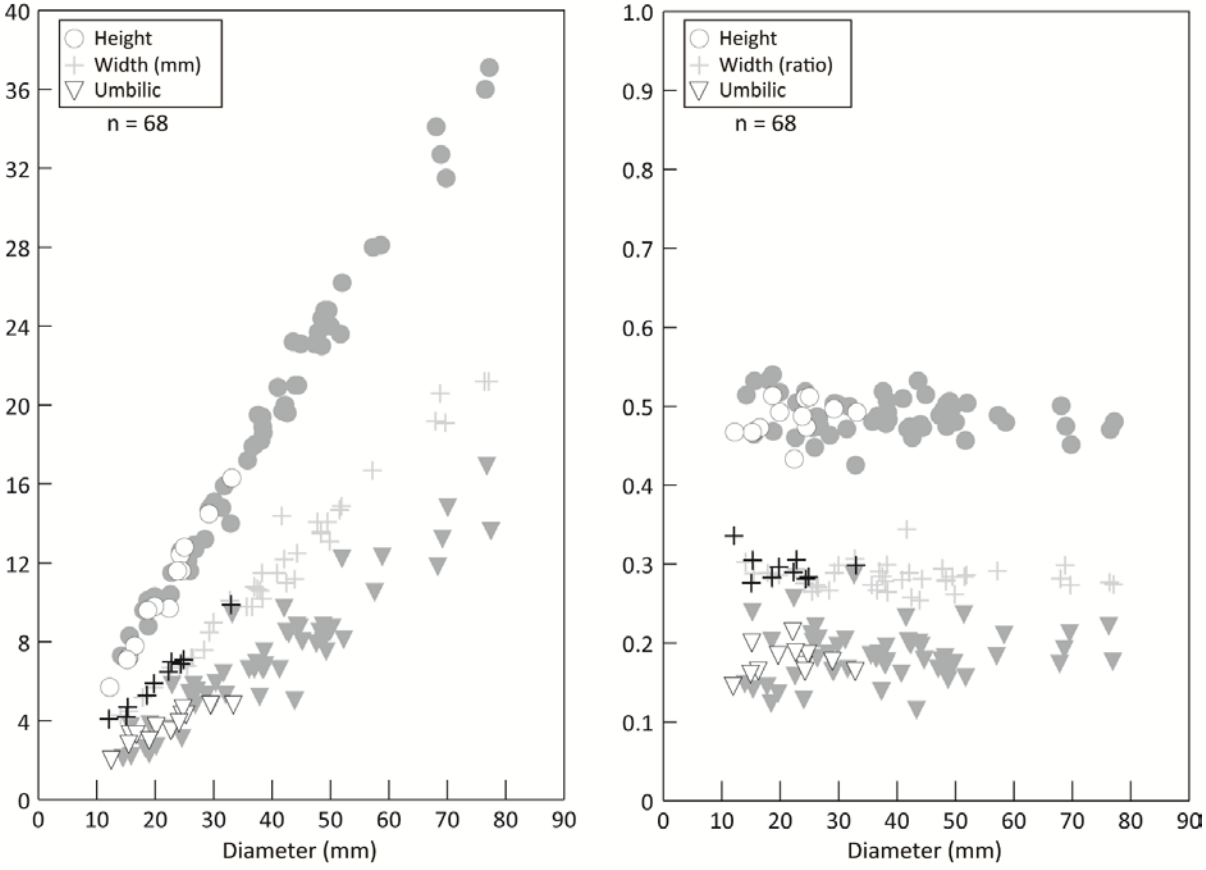

New middle and late Smithian ammonoid faunas from the Utah/Arizona border: new evidence for calibrating Early Triassic transgressive-regressive trends and paleobiogeographical signals in the western USA basin – Brayard et al.

Suppl. Fig. E. Scatter diagrams of H, W and U, and H/D, W/D and U/D for *Hemiprionites typus*. Open symbols indicate specimens from bed BRC, Workman Wash, Utah, early late Smithian (n = 6). Grey symbols indicate specimens from Palomino Ridge (data from Jattiot et al., 2017; n = 58) and Crittenden Springs (data from Jenks and Brayard, 2018; n = 23), Nevada.

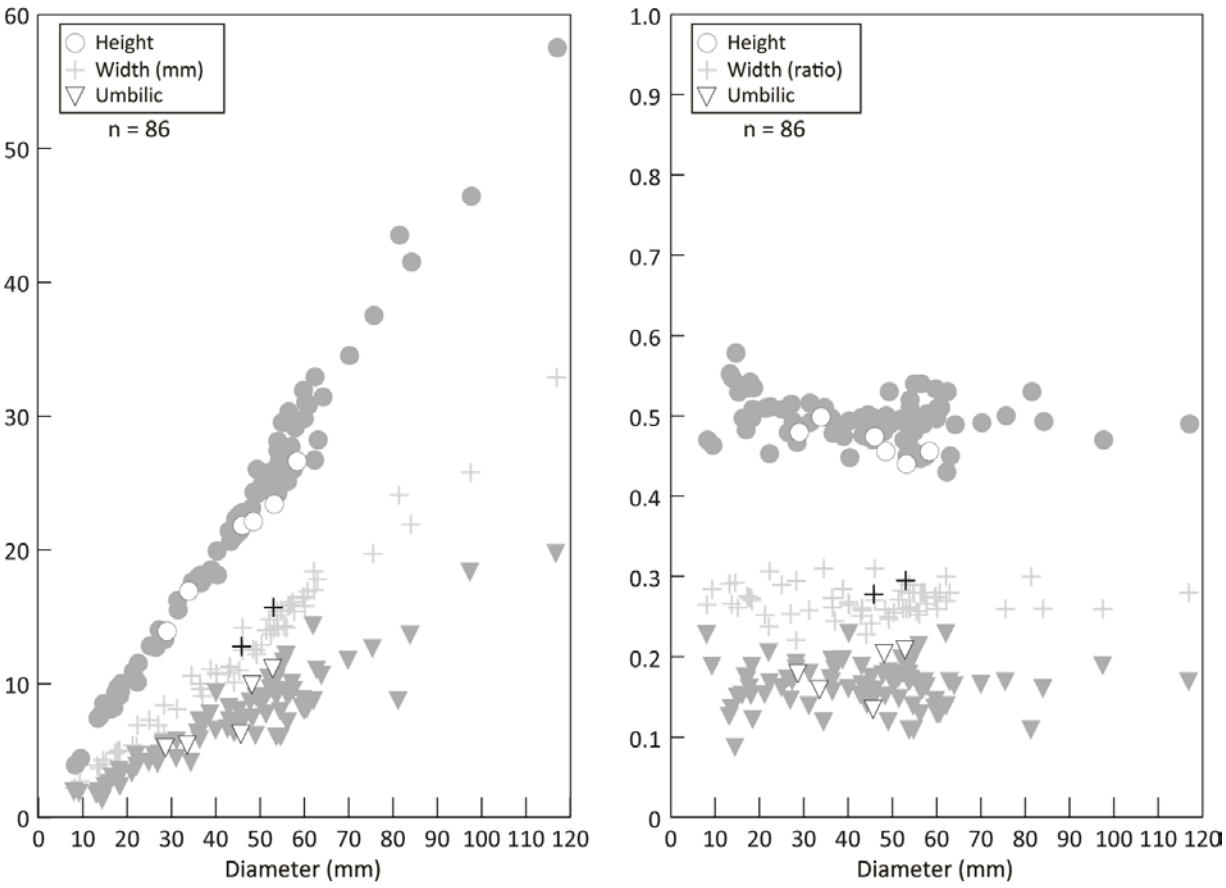

New middle and late Smithian ammonoid faunas from the Utah/Arizona border: new evidence for calibrating Early Triassic transgressive-regressive trends and paleobiogeographical signals in the western USA basin – Brayard et al.

Suppl. Fig. F. Scatter diagrams of H, W and U, and H/D, W/D and U/D for *Hemiprionites walcotti*. Open symbols indicate specimens from bed BRC, Workman Wash, Utah, early late Smithian (n = 5). Grey symbols indicate specimens from Palomino Ridge (data from Jattiot et al., 2017; n = 26) and Crittenden Springs (data from Jenks and Brayard, 2018; n = 2), Nevada.